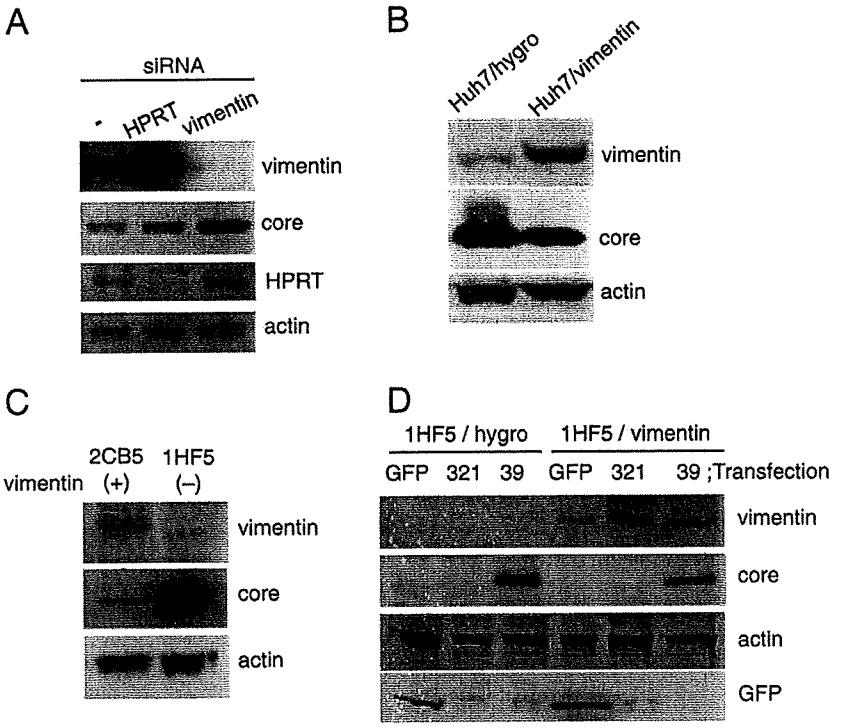

Fig. 3. Effects of cellular vimentin content on the level of expression of HCV core protein. Cellular level of expression of vimentin, HCV core protein, HPRT, β-actin, and GFP were analyzed by immunoblotting of total cell lysates (40 μg of protein) from various cells using specific antibodies. (A) Uc39-6 cells were transfected twice with a 2-day interval without (–) or with vimentin or control HPRT siRNA duplexes. Four days after the first transfection, cell lysates were collected and analyzed. (B) Huh7/hygro and Huh7/vimentin cells were transfected with the core protein-expression vector pcEF39neo, and selected under 1 mg/ml of G418 for 9 days. (C) The 2CB5 (vimentin+) and 1HF5 (vimentin–) lines of SW13 cells were transfected with pcEF39neo, and selected under 1 mg/ml of G418 for a week, followed by additional 2-week culture in normal culture medium. (D) 1HF5/hygro and 1HF5/vimentin cells were transfected with pcDNA3.1/EGFP (GFP), pcFE321swxneo (321), or pcEF39neo (39), and selected under 1 mg/ml of G418 for 9 days.

Under the various siRNA-treated conditions in Fig. 4, we also examined the protein levels of p53, one of the endogeneous host proteins the degradation of which is mainly regulated by proteasomal system (Morimoto et al., 2008). The pattern of p53 protein levels was very similar to that of core protein levels (Fig. 4), suggesting that the vimentin-dependent proteasomal degradation is not specific for the viral core protein. Vimentin-dependent proteasomal degradation system might be generally important for the turnover of endogeneous cellular proteins as well as the viral core protein.

Cellular vimentin contents affect HCV production

Since the level of expression of HCV core protein was affected by cellular vimentin content, we examined whether HCV production was also affected by cellular vimentin content. Infectious HCV (JFH1 strain) particles were used for the following infection assays. HCV production activity was determined by quantification of HCV core protein levels in the infected cells and culture supernatants. We first tested the effect of vimentin knockdown on HCV production. Examination of HCV-infected Huh7 cells treated with vimentin siRNA revealed higher amounts of HCV core protein in both cells and culture medium than examination of non-treated and control HPRT siRNA-treated cells (Fig. 5A). To examine whether the core protein levels in the cell-cultured media reflect the content of infectious HCV particles in them, Huh7 cells were treated with cell-cultured medium containing equal amounts (1.4 fmol) of the core protein collected from each type of cell described in Fig. 5A, and cellular levels of production of the core protein were determined by immunoblot analysis. They were nearly the same among the cells treated with each culture medium (Fig. 5B). These findings indicated that reduction of vimentin expression in Huh7 cells leads to more active HCV production and enhanced release to the supernatant.

We next examined the effects of vimentin overexpression on HCV production. When vimentin-overexpressing Huh7/vimentin and control Huh7/hygro cells were infected with HCV particles, Huh7/vimentin cells exhibited lower amounts of intracellular and extracellular HCV core protein than Huh7/hygro cells (Fig. 5C). Consistent with the results in Fig. 5A, these findings suggested that higher expression of vimentin in host cells resulted in lower HCV production.

We also examined the effect of vimentin knockdown on HCV RNA replication using a JFH1-subgenomic replicon (Fig. 5D). There were no significant differences in replication activities between vimentin-knocked-down cells and the other control cells. These findings indicated that cellular level of vimentin has no effects on HCV non-structural proteins which serve as a unit of RNA replication machinery of HCV. Collectively, these results demonstrated that HCV production activity but not HCV-RNA replication was inversely correlated with cellular vimentin content.

Table 1
mRNA levels of HCV core protein and β-actin in vimentin-knocked-down Uc39-6 cells

	siRNA		
	–	HPRT	vimentin
HCV core ($\times 10^4$ copies/μg total RNA)	2.9±0.3	1.7±0.1	3.0±0.2
β-actin ($\times 10^2$ copies/μg total RNA)	3.0±0.1	1.4±0.1	2.3±0.0
HCV core/β-actin[a]	1	1.3	1.3

Total RNA was isolated from Uc39-6 cells that had been treated twice with a 2-day interval with HPRT siRNA duplexes, with vimentin siRNA duplexes or without (–) either of them, and cultured for 4 days. mRNA levels of HCV core protein and β-actin (a control housekeeping gene) were determined by quantitative real-time PCR. Values are the mean±SD for three determinations.

[a] Numbers represent the relative amounts of HCV core protein mRNA normalized to β-actin level.

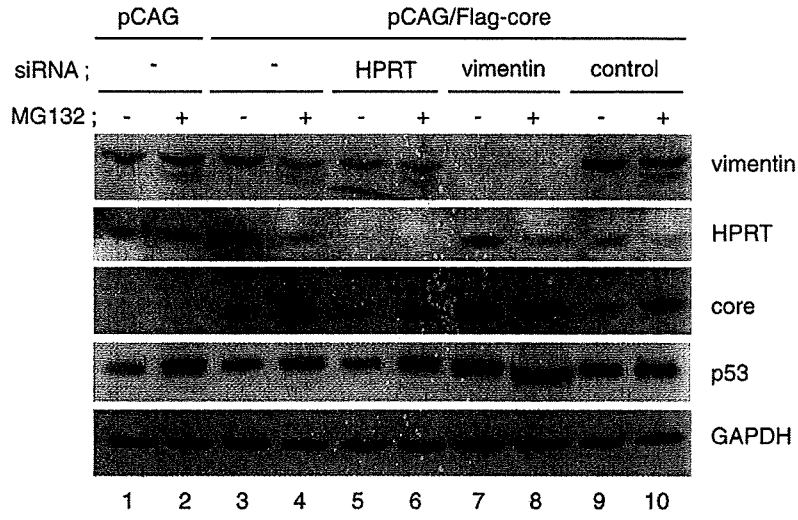

Fig. 4. Effects of the proteasome inhibitor MG132 on level of expression of HCV core protein in Huh7 cells. siRNA duplexes of control, HPRT, or vimentin, together with the core protein-expression vector pCAG/Flag-core, were transfected into Huh7 cells. After 2 days, transfection of these siRNAs was repeated. Cells were further cultured for 2 days and treated with (+) or without (−) MG132 (50 μM) for 16 h. Equivalent amounts of cell lysates were analyzed by immunoblotting with antibodies to vimentin, HPRT, core protein, p53, and GAPDH.

Furthermore, expression of vimentin and HCV core protein in Huh7 cells after HCV infection was observed by immunofluorescence microscopy (Fig. 5E), and the fluorescent intensity of vimentin in core-positive and core-negative Huh7 cells under HCV-infected conditions was determined (Fig. 5F). HCV-infected cells stained with the core-specific antibody always had lower vimentin content (Figs. 5E, F). Moreover, as shown in Fig. 5F, HCV core-negative cells exhibited more variable vimentin levels, whereas the core-positive cells had vimentin levels within a narrow range. These observations, which showed that a Huh7 cell population with lower vimentin content can preferentially produce HCV, were consistent with the results shown in Figs. 5A, C.

Finally, we examined the effects of MG132 on HCV core protein levels in HCV-infected cells in which vimentin was knocked-down or overexpressed. In the presence of MG132, non-treated and control HPRT siRNA-treated cells showed the significant increase of cellular HCV core protein levels, whereas vimentin-knocked-down cells did not (Fig. 5G). These results were consistent with those using HCV core-expressing cells (Fig. 4). HCV core content in vimentin-overexpressing Huh7/vimentin cells was lower than that in control Huh7/hygro cells, but after MG132 treatment Huh7/vimentin and Huh7/hygro cells showed the similar HCV core protein levels (Fig. 5H). Taken together, these results demonstrated the significant involvement of vimentin in proteasome-dependent degradation of HCV core protein in HCV-infected cells (Figs. 5G, H), as well as in HCV core-expressing cells (Fig. 4).

Discussion

By comparative proteomic analysis of the detergent-insoluble proteins in HCV core-expressing and non-expressing Huh7 cell lines, vimentin, an intermediate filament protein, was identified as the protein with the most dramatic reduction in level in the detergent-insoluble fraction of HCV core-expressing Uc39-6 cells (Figs. 1B and 2). On the other hand, there were no significant differences in the amounts of other major proteins including cytoskeletal components such as actin and cytokeratin 8/18 in the detergent-insoluble fractions between the core-expressing and non-expressing cells (Fig. 1B). These findings, together with similar results for other core-expressing cells (Fig. 2), suggested the existence of a specific relationship between the core protein and cellular vimentin. Consistent with these findings, immunofluorescence microscopic analysis of core-expressing cells (data not shown) and HCV-infected cells (Figs. 5E, F) showed that cells with intrinsic lower amount of vimentin are more permissive for higher HCV core protein content.

Knockdown of vimentin expression by siRNA treatment resulted in an increase in HCV core protein levels (Fig. 3A), while overexpression of vimentin reduced core protein contents (Fig. 3B). Similar results were obtained in the experiments using the vimentin-null cell line 1HF5 derived from SW13 cells (Figs. 3C and D). On the other hand, transient knockdown and overexpression of the core proteins in Uc39-6 and Huh7 cells, respectively, did not result in differences in cellular vimentin content (data not shown). These findings indicated that cellular vimentin level affects the level of expression of the core protein but not vice versa. Although transient expression of the core protein did not affect cellular vimentin content, why do various stable cell lines expressing the core protein have lower vimentin level? Since it was very hard to establish the cells stably expressing the core protein, we speculate that only the minor cell population innately having lower vimentin content was able to maintain the substantial core expression levels and was therefore selected.

We next demonstrated that vimentin affects core protein levels in post-translational fashion (Table 1) and is required for the proteasomal degradation of core protein in core-expressing cells (Fig. 4) and also in HCV-infected cells (Figs. 5G, H). Many studies with proteasome inhibitors have shown that a major pathway of degradation of core protein is mediated by the proteasomal system (Hope and McLauchlan, 2000; McLauchlan et al., 2002; Moriishi et al., 2003; Suzuki et al., 2001). PA28γ, a REG family proteasome activator also known as REGγ and Ki antigen, which is located in the nucleus, was shown to play an important role in the proteasomal degradation of the core protein (Moriishi et al., 2003). It was recently reported that the ubiquitin ligase E6AP, which is distributed in the perinuclear cytoplasm and colocalized with the core protein, is also involved in ubiquitylation and degradation of core protein (Shirakura et al., 2007). Vimentin filaments extend from the nuclear membrane toward the cell periphery. In addition, vimentin is known to colocalize with ubiquitinated protein aggregates and form aggresomes when the capacity of the proteasome is exceeded (Johnston et al., 1998). Pull-down assays against the core protein in core-expressing Huh7 cells indicated that a minor portion of cellular vimentin can interact with HCV core protein (data not shown), as

Kang et al. had reported previously (Kang et al., 2005). Co-staining of cellular vimentin and the core protein on immunofluorescence microscopy also supported the existence of a minor but definite association between them (data not shown). Based on these findings, we speculate that vimentin plays a role in the transport of the core protein to the nucleus, where it is then degraded, although further biochemical studies will be needed to demonstrate this.

HCV core protein is distributed mainly in the ER and lipid droplets in host cells (Barba et al., 1997), and the ER membrane associating the lipid droplets with core protein has been recognized as a site important for HCV production, particularly HCV RNA replication and virus particle assembly (Boulant et al., 2007; Miyanari et al., 2007). Vimentin is also closely associated with lipid droplets (Brasaemle et al., 2004; Lieber and Evans, 1996; Schweitzer and Evans, 1998). Thus, in addition to its degradative modulation of core protein, vimentin might also affect the function of lipid droplets and consequently inhibit HCV production. The effects of vimentin knock-down and overexpression on HCV production were actually stronger at the extracellular core protein level (secretion

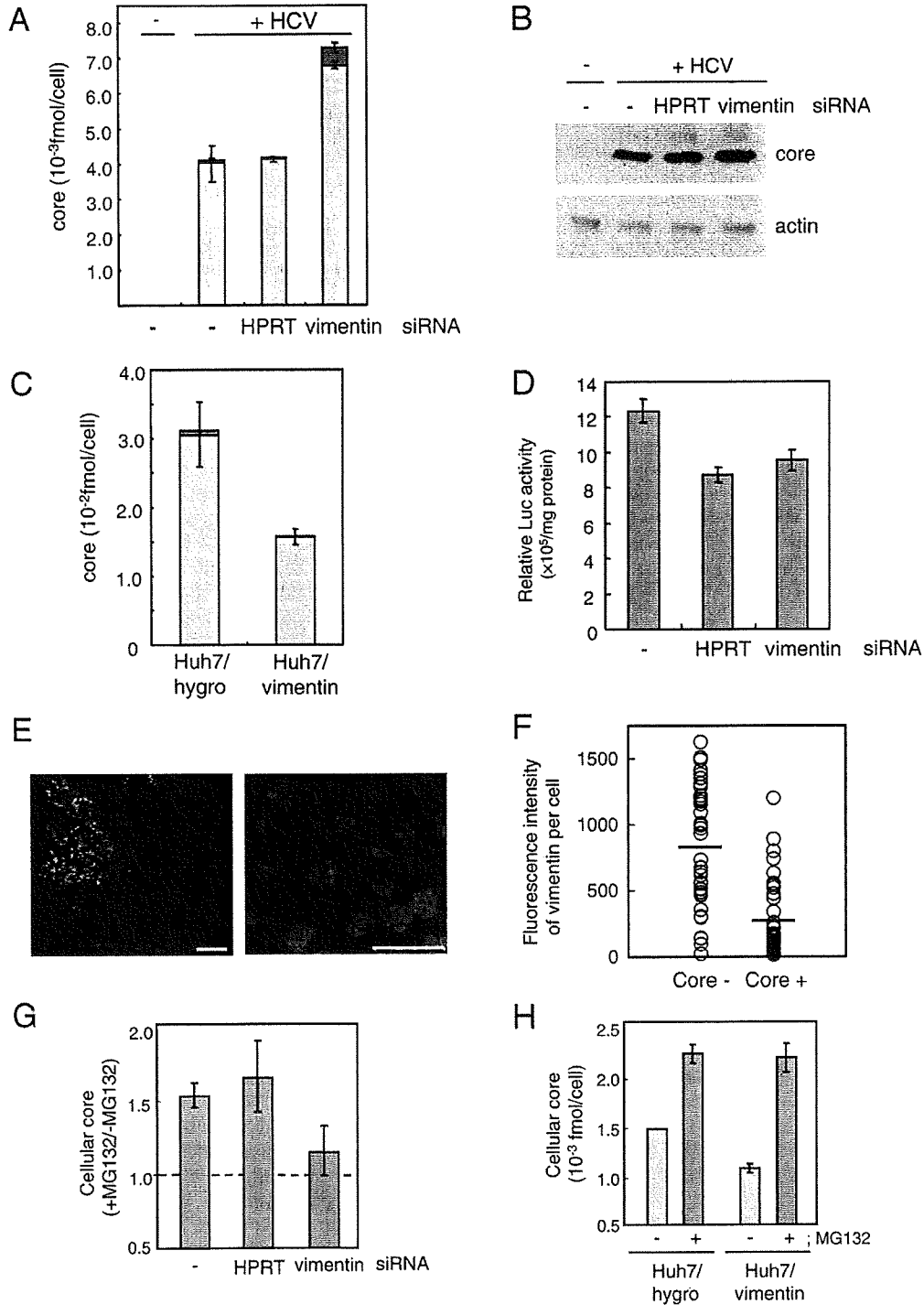

of the virus) than at the intracellular core protein level (Figs. 5A, C), suggesting additional activity of vimentin in the processes of HCV particle release.

Since the level of expression of vimentin in carcinomas is correlated with parameters of malignant potential such as tumor grade and tumor invasion, vimentin has been used as a marker of malignant tumors (Bannasch et al., 1982). It has indeed been reported that some HCV-infected patients with hepatocellular carcinoma exhibited up-regulation of vimentin expression in tumor tissue (Kim et al., 2003) although further statistical studies are required to clearly demonstrate this. Tanaka et al. noted that in livers of HCV-infected patients with hepatocelllular carcinoma the virus existed predominantly in non-cancerous tissue, at levels 10- to 100-fold higher than in cancerous tissue (Tanaka et al., 2004). These observations in human liver samples suggest that the reduction in HCV levels in hepatic tumor can be explained by the increase of vimentin expression in tumor, consistent with our findings for cultured cells.

In this study we demonstrated that cellular vimentin expression enhanced the proteasomal degradation of core protein and eventually restricted HCV production. Vimentin itself and sites of vimentin/core interaction may thus be novel targets of treatment using anti-HCV strategies.

Materials and methods

Antibodies

Mouse monoclonal antibodies to annexin II, fatty acid synthase, calnexin, lamin A/C, and GFP were purchased from BD Transduction Laboratories. Mouse monoclonal antibodies to HCV core protein, prohibitin, and glyceraldehyde-3-phosphate dehydrogenase (GAPDH) were from Anogen, Lab Vision, and Abcam, respectively. Rabbit polyclonal antibodies to vimentin, lamin B1, p53, and HPRT were from Santa Cruz Biotechnology Inc., while those to actin were from Biomedical Technologies Inc.

Plasmids

The mammalian expression vector of HCV core protein, pcEF39neo (Ruggieri et al., 1997), and the empty vector pcEF321swxneo (Harada et al., 1995) were described previously. The mammalian expression vector of Flag-tagged HCV core protein, pCAG/Flag-core, and the empty vector, pCAG, were described previously (Moriishi et al., 2003). For construction of a mammalian expression vector of vimentin, pcDNA3.1/Hygro/vimentin, vimentin fragment was amplified by PCR using the reverse-transcribed cDNAs of Huh7 cells as a template. The PCR primer pairs used were 5′-GCCATGTCCACCAGGTCCGTGTCC-3′ and 5′-TTATTATTCAAGGTCATCGTGATG-3′. The PCR products were inserted into the EcoRV site of pBluescript SKII(+). pBluescript SK(+)/vimentin was digested with Hind III and Xba I, and the vimentin fragment was inserted into pcDNA3.1/Hygro (Invitrogen), which had been digested with Hind III and Xba I. For construction of pcDNA3.1/EGFP, EGFP fragment was prepared by digestion of pEGFP-N1 (Clontech Laboratories, Inc.) with Nhe I and Hind III and inserted into pcDNA3.1/Hygro, which had been digested with Nhe I and Hind III. The subgenomic replicon constructs, pSGR-JFH1/Luc (wild type) and pSGR-JFH1/Luc-GND (GND mutation in the NS5B sequence), with the firefly luciferase reporter gene were described previously (Kato et al., 2005).

Cell lines

All hepatic cells used in this study were plated on collagen-coated dishes (Asahi Techno Glass, Japan). Human hepatic Huh7 and Huh7.5.1 cells were grown in normal culture medium [Dulbecco's modified Eagle's medium (DMEM) (KOJIN BIO, Japan) supplemented with 10% fetal bovine serum (FBS), 100 U/ml Penicillin G, and 100 mg/ml streptomycin sulfate] containing 0.1 mM non-essential amino acids (GIBCO) under a 5% CO_2 atmosphere at 37 °C. We used human hepatic cell lines constitutively expressing HCV core protein, including Hep39 from HepG2 cells (Harada et al., 1995; Ruggieri et al., 1997) and Uc39-2 and Uc39-6 from Huh7 cells (Fukasawa et al., 2006; Sato et al., 2006). Huh7 and HepG2 cell lines carrying the empty vector, Hepswx and Uc321, respectively, were used as a mock control. All of these stable transfectants were maintained in normal culture medium containing 1 mg/ml G418 (Sigma). The human adrenal carcinoma cell line SW13, the subtypes 2CB5 and 1HF5 of which do or do not express vimentin, respectively (Sarria et al., 1990), was maintained in normal culture medium. When the pcDNA3.1/EGFP vector was transfected into 2CB5 and 1HF5 cells, the percentage of GFP-positive cells was 56.3% and 53.6%, respectively, 2 days after transfection ($n=3$), indicating that there was no difference in the transfection efficiency between these cells. To establish vimentin-overexpressing cells, pcDNA3.1/Hygro/vimentin was transfected into 1HF5 and Huh7 cells using FuGENE 6 transfection regent (Roche). The vimentin-overexpressing Huh7 and 1HF5 cells were selected under hygromycin for 2 weeks and cloned to obtain Huh7/vimentin cells and 1HF5/vimentin cells, respectively. Huh7 and 1HF5 cells carrying the empty vector pcDNA/Hygro were also established, as Huh7/hygro cells and 1HF5/hygro cells, respectively.

Preparation of DISFs

Confluent monolayers of Uc321 and Uc39 cells in four culture dishes (150 mm inner diameter) were harvested by trypsinization, and 1.5×10^7 cells of each were pelleted by centrifugation (218 ×*g* for 5 min at 4 °C). After washing with PBS three times, each cell pellet was resuspended in 1 ml of lysis buffer [10 mM HEPES-HCl, pH 7.5, 10 mM NaCl, 140 mM KCl, 0.5 mM DTT, 0.5% Triton X-100 (Pierce Biotechnology), 10 mM NaF, Complete™ EDTA-free (Roche)] (i.e. a 20% cell suspension). The cell suspension was lysed with a ball-bearing homogenizer (Hope et al., 2002). The soluble fraction (designated the detergent-soluble fraction, DSF) containing ~85% of the total cellular proteins was collected by centrifugation of the cell

Fig. 5. HCV production in vimentin-knockdown and vimentin-overexpressing Huh7 cells. (A) Huh7 cells (5×10^4 cells) in 48-well plates were incubated with or without HCV particles (including 8.0 fmol of core protein) for 6 h, and then treated twice with a 3-day interval without (−) or with siRNA duplexes of HPRT or vimentin. After 7-day culture, the amounts of HCV core protein per cell in cells (light gray bar) and culture medium (dark gray bar) were determined. $n=3$. (B) Culture medium was collected at day 6 in the infection experiment described above in (A). The concentration of HCV core protein in these samples of medium was adjusted to 2.7 fmol/ml with fresh medium. Cells were infected with these samples of medium containing 1.4 fmol of HCV core protein for 2 days, and harvested after 7-day incubation. Infectivity was analyzed by the immunoblotting of cell lysates with antibodies to HCV core protein and β-actin. (C) Vimentin-overexpressing Huh7/vimentin and control Huh7/hygro cells infected with HCV were harvested after 7-day incubation. The amounts of HCV core protein per cell in cells (light gray bar) and culture medium (dark gray bar) were determined. (D) Huh7 cells harboring the HCV subgenomic replicon containing a luciferase reporter gene were transfected without (−) or with siRNA duplexes of HPRT or vimentin. After 2.5-day culture, luciferase activity in cell extracts was determined. $n=3$. (E) Immunofluorescence microscopic analysis of HCV-infected Huh7 cells. After infection with HCV, Huh7 cells were cultured for 6 days. HCV core protein (green) and vimentin (red) were then detected with specific antibodies. Nuclei (blue) were stained with DAPI. Two views showing low and high magnifications are displayed. Bars, 100 μm in the left panel; 50 μm in the right panel. (F) Under the HCV-infected conditions in panel E, fluorescence intensity of vimentin in core-positive and core-negative Huh7 cells was determined by line profile analysis. $n=40$. Statistical significance of differences in fluorescence intensity of vimentin between core-positive and core-negative cells was evaluated using Student's *t* test, showing $p<10^{-8}$. (G) As in (A), Huh7 cells were incubated with HCV particles, and then treated twice with a 2-day interval without (−) or with siRNA duplexes of HPRT or vimentin. After 4.5-day culture, cells were treated with (+) or without (−) MG132 (50 μM) for 16 h. In each culture condition, the ratio of HCV core protein level in the MG132-treated cells to that in MG132-untreated cells was determined. $n=3$. (H) Huh7/vimentin and Huh7/hygro cells infected with HCV were cultured for 4 days and treated with (+) or without (−) MG132 (50 μM) for 16 h. The amounts of cellular core protein per cell were determined. $n=3$.

lysate performed twice at 218 ×g for 5 min at 4 °C. The insoluble pellet was suspended in 2 ml of lysis buffer containing 1.62 M sucrose and then centrifuged at 10,000 ×g for 1 h at 4 °C. The pellet was resuspended in 1 ml of lysis buffer containing 1.0 M sucrose and layered over 2 ml of lysis buffer containing 2.0 M sucrose. After centrifugation at 50,000 ×g for 2 h at 4 °C, the precipitated fraction containing ~15% of total cellular proteins was collected and resuspended in lysis buffer containing 0.25 M sucrose at a concentration of 3 mg protein/ml (designated the detergent-insoluble fraction, DISF). Each fraction was stored at −80 °C until use. The protein concentrations in these preparations were determined with BCA protein assay reagents (Pierce Biotechnology) using BSA as a standard.

2D-PAGE/MALDI-QIT-TOF MS analysis

The DISF (0.15 mg protein) of each cell line was cleaned using a PlusOne™ 2-D Clean Up kit (GE Healthcare) and resuspended in rehydration solution containing 9 M urea, 4% CHAPS, 65 mM dithioerythritol, and 0.5% ampholyte. The first-dimensional IEF was performed with an Immobiline Dry Strip pH 4–7 according to the manufacturer's instruction (GE Healthcare). The second-dimensional electrophoresis was carried out on 12% SDS-polyacrylamide gel, and the gel was stained with SYPRO-Ruby (Bio-Rad). Spot detection and comparison in 2D images were accomplished with PDQuest™ 2-D analysis software ver. 7.3 (Bio-Rad). The protein bands were excised from the gel and subjected to in-gel trypsin digestion. The tryptic peptide mixtures were analyzed by MALDI-QIT-TOF MS (AXIMA-QIT, Shimazu Biotech, Japan) as described previously (Sato et al., 2006; Shevchenko et al., 1996). Mascot software (Matrix Science) was used for protein identification.

Immunoblot analysis

The proteins were separated by electrophoresis in precast NuPAGE 10% or 12% Bis–Tris gels (Invitrogen), and then transferred to a polyvinylidene difluoride membrane. The membranes were blocked overnight at 4 °C or for 60 min at room temperature in Tris-buffered saline containing 0.1% Tween 20 and 5% skim milk. The blots were probed with the first antibodies at 1:1000 dilution for 60 min at room temperature and then incubated with horseradish peroxidase (HRP)-conjugated goat anti-rabbit IgG (Bio-Rad) or HRP-conjugated goat anti-mouse IgG (GE Healthcare) at 1:2000 dilution for 45 min. Detection of immunoreactive proteins was performed using an ECL system (GE Healthcare).

Quantitative real-time PCR analysis

Cellular total RNAs were prepared with an RNeasy kit (Qiagen). The total RNA fraction (1 μg) was processed directly to cDNA using a Transcriptor First Strand cDNA Synthesis Kit (Roche). Of the total 20 μl cDNA solution, an aliquot of 0.5–2 μl was used for each real-time PCR assay. The PCR primers used for HCV core protein were: forward, 5′-AGGAAGACTTCCGAGCG-3′, and reverse, 5′-GGGTGACAGGAGCCATC-3′. The PCR primers for actin were obtained from the LightCycler™-Primer Set (Roche). Quantitative real-time PCR was carried out in a LightCycler (Roche) using LightCycler-FastStart DNA Master SYBR Green I (Roche).

Transfection of siRNA

Subconfluent cells cultured in a 48-well plate were transfected twice at a 2- or 3-day interval with 30 nM of vimentin-specific, HPRT-specific, or negative control (Invitrogen) siRNA duplexes using Lipofectamine RNAiMAX (Invitrogen) following the manufacturer's instructions. The siRNA target sequences were as follows: vimentin (sense), 5′-ACCTTGAACGCAAAGTGGAATCTTT-3′; HPRT-S1 (sense), 5′-AAGCCAGACUUUGUUGGAUUUGAAA-3′.

Infection of Huh7 cells with HCV

Infectious HCV (JFH1 strain) particles were produced in Huh7.5.1 cells as described previously (Wakita et al., 2005). Culture supernatant containing infectious HCV particles was collected and stored at −80 °C until use. Subconfluent naïve Huh7, Huh7/hygro, or Huh7/vimentin cells in 24-well or 48-well plates were exposed to normal culture medium containing HCV particles (1.4–8 fmol core protein/well, corresponding to moi=0.0175–0.1) for 6 h at 37 °C. Cells were then washed and maintained in 500 μl (24-well) or 250 μl (48-well) of normal culture medium for 6–7 days at 37 °C. To determine HCV production activity, the amounts of HCV core protein in the culture medium and cell lysates were quantified with an enzyme-linked immunosorbent assay (ELISA) (Ortho® HCV antigen ELISA test, Ortho-Clinical Diagnostics, Japan).

Assay for activity of HCV genomic RNA replication

The RNAs (30 μg) transcribed from pSGR-JFH1/Luc and pSGR-JFH1/Luc-GND (Kato et al., 2005) were transfected into Huh7 cells (1.6×10^6 cells) by electroporation. Transfected cells in normal culture medium were immediately seeded into 48-well plates at 9.0×10^4 cells/well. Four hours after transfection, siRNAs were also transfected into these cells. After incubation for 2.5 days, cells were harvested and the luciferase activity in cell lysates was determined with the Luciferase Assay System (Promega). Since the luciferase activities of the JFH1/Luc replicon were ~400-fold higher than those of the JFH1/Luc-GND mutant replicon, background luciferase activity, which is independent of replication activity, was very low in our experimental conditions.

Immunofluorescence microscopy

Cells cultured on glass cover slips (in 24-well plates) were fixed in 1% formaldehyde-PBS for 1 h at 4 °C, permeabilized in PBS containing 0.1% Triton X-100 for 5 min, and washed twice with PBS. The cell monolayers were incubated with rabbit anti-vimentin antibodies (1:100) and mouse anti-HCV core protein antibodies (1:100) for 60 min at room temperature. After washing with PBS, the cells were incubated with Alexa488-conjugated anti-mouse IgG, Alexa594-conjugated anti-rabbit IgG, and DAPI (4′, 6′-diamidino-2-phenylindole) (Invitrogen) for 60 min at 4 °C. Coverslips were washed with PBS and mounted on glass slides. Immunofluorescence was visualized and quantitated with a confocal laser-scanning microscope (Axiovert 100M, Carl Zeiss) equipped with a LSM510 system (Carl Zeiss).

Acknowledgments

Huh-7.5.1 cells and Huh-7 cells were kindly provided by F. V. Chisari (Scripps Research Institute).

This work was supported in part by grants-in-aid from the Ministry of Health, Labor, and Welfare of Japan, and by grants-in-aid from the Ministry of Education, Culture, Sports, Science, and Technology of Japan.

References

Aizaki, H., Lee, K.J., Sung, V.M., Ishiko, H., Lai, M.M., 2004. Characterization of the hepatitis C virus RNA replication complex associated with lipid rafts. Virology 324 (2), 450–461.

Ariumi, Y., Kuroki, M., Abe, K., Dansako, H., Ikeda, M., Wakita, T., Kato, N., 2007. DDX3 DEAD-box RNA helicase is required for hepatitis C virus RNA replication. J. Virol. 81 (24), 13922–13926.

Bannasch, P., Zerban, H., Mayer, D., 1982. The cytoskeleton in tumor cells. Pathol. Res. Pract. 175 (2–3), 196–211.

Barba, G., Harper, F., Harada, T., Kohara, M., Goulinet, S., Matsuura, Y., Eder, G., Schaff, Z., Chapman, M.J., Miyamura, T., Brechot, C., 1997. Hepatitis C virus core protein shows a cytoplasmic localization and associates to cellular lipid storage droplets. Proc. Natl. Acad. Sci. U. S. A. 94 (4), 1200–1205.

Bartenschlager, R., Lohmann, V., 2000. Replication of hepatitis C virus. J. Gen. Virol. 81 (Pt 7), 1631–1648.
Boulant, S., Targett-Adams, P., McLauchlan, J., 2007. Disrupting the association of hepatitis C virus core protein with lipid droplets correlates with a loss in production of infectious virus. J. Gen. Virol. 88 (Pt 8), 2204–2213.
Brasaemle, D.L., Dolios, G., Shapiro, L., Wang, R., 2004. Proteomic analysis of proteins associated with lipid droplets of basal and lipolytically stimulated 3T3-L1 adipocytes. J. Biol. Chem. 279 (45), 46835–46842.
Choo, Q.L., Kuo, G., Weiner, A.J., Overby, L.R., Bradley, D.W., Houghton, M., 1989. Isolation of a cDNA clone derived from a blood-borne non-A, non-B viral hepatitis genome. Science 244 (4902), 359–362.
Fukasawa, M., Tanaka, Y., Sato, S., Ono, Y., Nitahara-Kasahara, Y., Suzuki, T., Miyamura, T., Hanada, K., Nishijima, M., 2006. Enhancement of de novo fatty acid biosynthesis in hepatic cell line Huh7 expressing hepatitis C virus core protein. Biol. Pharm. Bull. 29 (9), 1958–1961.
Harada, T., Kim, D.W., Sagawa, K., Suzuki, T., Takahashi, K., Saito, I., Matsuura, Y., Miyamura, T., 1995. Characterization of an established human hepatoma cell line constitutively expressing non-structural proteins of hepatitis C virus by transfection of viral cDNA. J. Gen. Virol. 76 (Pt 5), 1215–1221.
Hope, R.G., McLauchlan, J., 2000. Sequence motifs required for lipid droplet association and protein stability are unique to the hepatitis C virus core protein. J. Gen. Virol. 81 (Pt 8), 1913–1925.
Hope, R.G., Murphy, D.J., McLauchlan, J., 2002. The domains required to direct core proteins of hepatitis C virus and GB virus-B to lipid droplets share common features with plant oleosin proteins. J. Biol. Chem. 277 (6), 4261–4270.
Johnston, J.A., Ward, C.L., Kopito, R.R., 1998. Aggresomes: a cellular response to misfolded proteins. J. Cell Biol. 143 (7), 1883–1898.
Kang, S.M., Shin, M.J., Kim, J.H., Oh, J.W., 2005. Proteomic profiling of cellular proteins interacting with the hepatitis C virus core protein. Proteomics 5 (8), 2227–2237.
Kato, T., Date, T., Miyamoto, M., Sugiyama, M., Tanaka, Y., Orito, E., Ohno, T., Sugihara, K., Hasegawa, I., Fujiwara, K., Ito, K., Ozasa, A., Mizokami, M., Wakita, T., 2005. Detection of anti-hepatitis C virus effects of interferon and ribavirin by a sensitive replicon system. J. Clin. Microbiol. 43 (11), 5679–5684.
Kim, W., Oe Lim, S., Kim, J.S., Ryu, Y.H., Byeon, J.Y., Kim, H.J., Kim, Y.I., Heo, J.S., Park, Y.M., Jung, G., 2003. Comparison of proteome between hepatitis B virus- and hepatitis C virus-associated hepatocellular carcinoma. Clin. Cancer Res. 9 (15), 5493–5500.
Kuo, G., Choo, Q.L., Alter, H.J., Gitnick, G.L., Redeker, A.G., Purcell, R.H., Miyamura, T., Dienstag, J.L., Alter, M.J., Stevens, C.E., et al., 1989. An assay for circulating antibodies to a major etiologic virus of human non-A, non-B hepatitis. Science 244 (4902), 362–364.
Lieber, J.G., Evans, R.M., 1996. Disruption of the vimentin intermediate filament system during adipose conversion of 3T3-L1 cells inhibits lipid droplet accumulation. J. Cell. Sci. 109 (Pt 13), 3047–3058.
Matto, M., Rice, C.M., Aroeti, B., Glenn, J.S., 2004. Hepatitis C virus core protein associates with detergent-resistant membranes distinct from classical plasma membrane rafts. J. Virol. 78 (21), 12047–12053.
McLauchlan, J., Lemberg, M.K., Hope, G., Martoglio, B., 2002. Intramembrane proteolysis promotes trafficking of hepatitis C virus core protein to lipid droplets. EMBO J. 21 (15), 3980–3988.
Miyanari, Y., Atsuzawa, K., Usuda, N., Watashi, K., Hishiki, T., Zayas, M., Bartenschlager, R., Wakita, T., Hijikata, M., Shimotohno, K., 2007. The lipid droplet is an important organelle for hepatitis C virus production. Nat. Cell Biol. 9 (9), 1089–1097.
Moriishi, K., Okabayashi, T., Nakai, K., Moriya, K., Koike, K., Murata, S., Chiba, T., Tanaka, K., Suzuki, R., Suzuki, T., Miyamura, T., Matsuura, Y., 2003. Proteasome activator PA28gamma-dependent nuclear retention and degradation of hepatitis C virus core protein. J. Virol. 77 (19), 10237–10249.
Morimoto, T., Fujita, M., Kawamura, T., Sunagawa, Y., Takaya, T., Wada, H., Shimatsu, A., Kita, T., Hasegawa, K., 2008. Myocardial regulation of p300 and p53 by doxorubicin involves ubiquitin pathways. Circ. J. 72 (9), 1506–1511.
Moriya, K., Yotsuyanagi, H., Shintani, Y., Fujie, H., Ishibashi, K., Matsuura, Y., Miyamura, T., Koike, K., 1997. Hepatitis C virus core protein induces hepatic steatosis in transgenic mice. J. Gen. Virol. 78 (Pt 7), 1527–1531.
Moriya, K., Fujie, H., Shintani, Y., Yotsuyanagi, H., Tsutsumi, T., Ishibashi, K., Matsuura, Y., Kimura, S., Miyamura, T., Koike, K., 1998. The core protein of hepatitis C virus induces hepatocellular carcinoma in transgenic mice. Nat. Med. 4 (9), 1065–1067.
Randall, G., Panis, M., Cooper, J.D., Tellinghuisen, T.L., Sukhodolets, K.E., Pfeffer, S., Landthaler, M., Landgraf, P., Kan, S., Lindenbach, B.D., Chien, M., Weir, D.B., Russo, J.J., Ju, J., Brownstein, M.J., Sheridan, R., Sander, C., Zavolan, M., Tuschl, T., Rice, C.M., 2007. Cellular cofactors affecting hepatitis C virus infection and replication. Proc. Natl. Acad. Sci. U. S. A. 104 (31), 12884–12889.
Reed, K.E., Rice, C.M., 2000. Overview of hepatitis C virus genome structure, polyprotein processing, and protein properties. Curr. Top. Microbiol. Immunol. 242, 55–84.
Ruggieri, A., Harada, T., Matsuura, Y., Miyamura, T., 1997. Sensitization to Fas-mediated apoptosis by hepatitis C virus core protein. Virology 229 (1), 68–76.
Sarria, A.J., Nordeen, S.K., Evans, R.M., 1990. Regulated expression of vimentin cDNA in cells in the presence and absence of a preexisting vimentin filament network. J. Cell Biol. 111 (2), 553–565.
Sato, S., Fukasawa, M., Yamakawa, Y., Natsume, T., Suzuki, T., Shoji, I., Aizaki, H., Miyamura, T., Nishijima, M., 2006. Proteomic profiling of lipid droplet proteins in hepatoma cell lines expressing hepatitis C virus core protein. J. Biochem. (Tokyo) 139 (5), 921–930.
Schweitzer, S.C., Evans, R.M., 1998. Vimentin and lipid metabolism. Sub-cell. Biochem. 31, 437–462.
Shevchenko, A., Wilm, M., Vorm, O., Jensen, O.N., Podtelejnikov, A.V., Neubauer, G., Shevchenko, A., Mortensen, P., Mann, M., 1996. A strategy for identifying gel-separated proteins in sequence databases by MS alone. Biochem. Soc. Trans. 24 (3), 893–896.
Shi, S.T., Lee, K.J., Aizaki, H., Hwang, S.B., Lai, M.M., 2003. Hepatitis C virus RNA replication occurs on a detergent-resistant membrane that cofractionates with caveolin-2. J. Virol. 77 (7), 4160–4168.
Shirakura, M., Murakami, K., Ichimura, T., Suzuki, R., Shimoji, T., Fukuda, K., Abe, K., Sato, S., Fukasawa, M., Yamakawa, Y., Nishijima, M., Moriishi, K., Matsuura, Y., Wakita, T., Suzuki, T., Howley, P.M., Miyamura, T., Shoji, I., 2007. E6AP ubiquitin ligase mediates ubiquitylation and degradation of hepatitis C virus core protein. J. Virol. 81 (3), 1174–1185.
Suzuki, R., Tamura, K., Li, J., Ishii, K., Matsuura, Y., Miyamura, T., Suzuki, T., 2001. Ubiquitin-mediated degradation of hepatitis C virus core protein is regulated by processing at its carboxyl terminus. Virology 280 (2), 301–309.
Suzuki, T., Ishii, K., Aizaki, H., Wakita, T., 2007. Hepatitis C viral life cycle. Adv. Drug Deliv. Rev. 59 (12), 1200–1212.
Tanaka, T., Inoue, K., Hayashi, Y., Abe, A., Tsukiyama-Kohara, K., Nuriya, H., Aoki, Y., Kawaguchi, R., Kubota, K., Yoshiba, M., Koike, M., Tanaka, S., Kohara, M., 2004. Virological significance of low-level hepatitis B virus infection in patients with hepatitis C virus associated liver disease. J. Med. Virol. 72 (2), 223–229.
Wakita, T., Pietschmann, T., Kato, T., Date, T., Miyamoto, M., Zhao, Z., Murthy, K., Habermann, A., Krausslich, H.G., Mizokami, M., Bartenschlager, R., Liang, T.J., 2005. Production of infectious hepatitis C virus in tissue culture from a cloned viral genome. Nat. Med. 11 (7), 791–796.

JOURNAL OF VIROLOGY, June 2008, p. 5715–5724 Vol. 82, No. 12
0022-538X/08/$08.00+0 doi:10.1128/JVI.02530-07

Critical Role of Virion-Associated Cholesterol and Sphingolipid in Hepatitis C Virus Infection▽

Hideki Aizaki,[1] Kenichi Morikawa,[1] Masayoshi Fukasawa,[2] Hiromichi Hara,[1] Yasushi Inoue,[1] Hideki Tani,[3] Kyoko Saito,[2] Masahiro Nishijima,[2] Kentaro Hanada,[2] Yoshiharu Matsuura,[3] Michael M. C. Lai,[4] Tatsuo Miyamura,[1] Takaji Wakita,[1] and Tetsuro Suzuki[1]*

Department of Virology II[1] and Department of Biochemistry and Cell Biology,[2] National Institute of Infectious Diseases, Tokyo 162-8640, and Department of Molecular Virology, Research Institute for Microbial Diseases, Osaka University, Osaka 565-0871,[3] Japan, and Department of Molecular Microbiology and Immunology, University of Southern California, Los Angeles, California 90033-1054[4]

Received 27 November 2007/Accepted 17 March 2008

In this study, we establish that cholesterol and sphingolipid associated with hepatitis C virus (HCV) particles are important for virion maturation and infectivity. In a recently developed culture system enabling study of the complete life cycle of HCV, mature virions were enriched with cholesterol as assessed by the molar ratio of cholesterol to phospholipid in virion and cell membranes. Depletion of cholesterol from the virus or hydrolysis of virion-associated sphingomyelin almost completely abolished HCV infectivity. Supplementation of cholesterol-depleted virus with exogenous cholesterol enhanced infectivity to a level equivalent to that of the untreated control. Cholesterol-depleted or sphingomyelin-hydrolyzed virus had markedly defective internalization, but no influence on cell attachment was observed. Significant portions of HCV structural proteins partitioned into cellular detergent-resistant, lipid-raft-like membranes. Combined with the observation that inhibitors of the sphingolipid biosynthetic pathway block virion production, but not RNA accumulation, in a JFH-1 isolate, our findings suggest that alteration of the lipid composition of HCV particles might be a useful approach in the design of anti-HCV therapy.

Hepatitis C virus (HCV) is recognized as a major cause of chronic liver disease, including chronic hepatitis, hepatic steatosis, cirrhosis, and hepatocellular carcinoma. It presently affects approximately 200 million people worldwide (26). HCV is an enveloped positive-strand RNA virus belonging to the *Hepacivirus* genus of the family *Flaviviridae*. Its genome of ~9.6 kb encodes a polyprotein precursor of ~3,000 residues, and the structural proteins (core, E1, and E2) reside in its N-terminal region.

Little is known about the assembly of HCV and its virion structure, because efficient production of authentic HCV particles has only recently been achieved. Nucleocapsid assembly generally involves oligomerization of the capsid protein and encapsidation of genomic RNA. This process is thought to occur upon interaction of the core protein with viral RNA, and this core-RNA interaction may induce a change from RNA replication to packaging. As with related viruses, the mature HCV virion likely consists of a nucleocapsid and an outer envelope composed of a lipid membrane and envelope proteins. Expression of the structural proteins in mammalian cells has been observed to generate virus-like particles with ultrastructural properties similar to those of HCV virions (5, 29). Packaging of these HCV-like particles into intracellular vesicles as a result of budding from the endoplasmic reticulum (ER) has also been observed (8, 34). However, HCV structural proteins are observed both in the ER and in the Golgi apparatus (45). Moreover, complex N-linked glycans have been detected on the surfaces of HCV particles isolated from patient sera, suggesting that the glycans transit through the Golgi apparatus (44). Interactions between the core and E1/E2 proteins are thought to determine viral morphology and are mediated through a cytoplasmic loop present in the polytopic form of E1 (35). Recently, we and others have identified a unique HCV genotype 2a isolate, JFH-1, that is able to replicate and produce high levels of infectious virus in culture (HCVcc) (54, 56), enabling us to investigate new aspects of the HCV life cycle.

In this study, we examine the importance of cholesterol and sphingolipid in association with the HCV membrane in virion maturation and virus infectivity. Mature HCV particles are rich in cholesterol. Cholesterol depletion or hydrolysis of sphingolipid from HCV particles results in a loss of infectivity. We further demonstrate a requirement for virion-associated cholesterol and sphingolipid for viral entry.

MATERIALS AND METHODS

Cell culture. The human hepatoma cell line Huh-7, which is permissive to HCV infection, was obtained from Francis V. Chisari (The Scripps Research Institute). Human embryonic kidney 293T cells were cultured in Dulbecco's modified Eagle medium (DMEM)–10% fetal bovine serum. Huh-7 cell lines, which carry subgenomic replicon RNA of either the JFH-1 (20) or the N (11, 17) strain, were cultured as previously described (21, 46).

Reagents. The primary antibodies used in this study were mouse monoclonal antibodies against vesicular stomatitis virus glycoprotein (VSV-G) (Sigma, St. Louis, MO), HCV E1 (54) and E2 (Biodesign International, Saco, ME), caveolin-2 (New England Biolabs, Beverly, MA), and CD81 (BD Pharmingen, Franklin Lakes, NJ), as well as rabbit polyclonal antibodies against calnexin (Stressgen, Ann Arbor, MI) and HCV core (48). ISP-1/myriocin, cholesterol, and

* Corresponding author. Mailing address: Department of Virology II, National Institute of Infectious Diseases, 1-23-1 Toyama, Shinjuku-ku, Tokyo 162-8640, Japan. Phone: 81 3 5285 1111. Fax: 81 3 5285 1161. E-mail: tesuzuki@nih.go.jp.

▽ Published ahead of print on 26 March 2008.

heparinase I were purchased from Sigma, and recombinant *Bacillus cereus* sphingomyelinase (SMase) was obtained from Higeta Shoyu (Tokyo, Japan). (1*R*,3*R*)-*N*-(3-Hydroxy-1-hydroxymethyl-3-phenylpropyl) dodecanamide (HPA-12), which was synthesized as described elsewhere (24), was a gift from Shu Kobayashi (University of Tokyo).

Plasmids. pCAE1 and pCAE2 contain HCV cDNAs spanning the E1 region (amino acids 192 to 383) with a FLAG tag at the N terminus and the E2 region (amino acids 384 to 809) with a Myc tag at the N terminus of strain NIHJ1 (1), respectively, under the control of the CAG promoter (38). pCAV340V and pCAV711V consist of the ectodomains of E1 and E2, respectively, with the N-terminal signal sequences, transmembrane domains, and cytoplasmic domains derived from VSV-G, as described elsewhere (50) (see Fig. 4D).

Virus production. Plasmid pJFH1, containing full-length cDNA of the JFH-1 isolate, was used to generate HCVcc as described elsewhere (23, 33, 34, 54). pJ6/JFH was obtained from JFH1 by replacement of the 5′ untranslated region to the p7 region (EcoRI-BclI) of J6. In vitro-transcribed RNA from linearized pJFH1 or pJ6/JFH1 was delivered to Huh-7 cells by electroporation. Culture supernatants were collected at 72 h posttransfection, clarified by low-speed centrifugation, passed through a 0.45-mm-pore-size filter, and concentrated using an Amicon Ultra-15 unit (Millipore, Bedford, MA) or by ultracentrifugation (23). Infectious titers, HCV RNA copies, and core protein concentrations of the viral stocks were $\sim 5 \times 10^3$ focus-forming units per ml, $\sim 1 \times 10^7$ copies/ml, and $\sim 1 \times 10^4$ fmol/liter, respectively. HCVcc was isolated by a combination of ultrafiltration, ion-exchange chromatography, heparin affinity chromatography, and sucrose density ultracentrifugation (33; K. Morikawa and T. Wakita, unpublished data). Pseudotyped VSV containing E1 and E2 proteins of the HCV genotype 1a isolate H77c (HCVpv) was generated as previously described (51). Briefly, 293T cells transiently expressing E1 and E2 proteins (strain H77) were infected with VSVdelG-GFP/G, in which the G envelope gene was replaced with green fluorescent protein (GFP) and pseudotyped with VSV-G.

Determination of cholesterol and phospholipid contents of HCVcc and infected cells. Cellular and viral lipids were extracted from isolated HCVcc and from uninfected and infected Huh-7 cells. Cholesterol content was determined using the cholesterol oxidase method as previously described (14). Total phospholipid content was determined using the method of Rouser et al. (42).

Cholesterol depletion and replacement. To remove cholesterol from the HCV envelope, stock samples of HCVcc were treated with *methyl*-β-cyclodextrin (B-CD) in DMEM (Sigma) supplemented with 10% fetal bovine serum (Sigma) and nonessential amino acids (Invitrogen, Carlsbad, CA) for 1 h at 37°C, followed by centrifugation at 100,000 × *g* for 3 h to form a pellet, which was resuspended in 0.5 ml of the medium. In order to replenish cholesterol, the medium of HCVcc treated with 5 mg/ml B-CD was replaced with DMEM containing various concentrations of exogenous cholesterol (Sigma) and incubated for 1 h, followed by centrifugation to form a pellet. In order to perform HCVcc infection assays, Huh-7 cells were infected with HCVcc, with or without the treatment described above, for 1 h at 37°C and then washed as described above. Viral core protein levels in the cells and in the supernatant were quantified 72 h later using an HCV core enzyme-linked immunosorbent assay (Ortho-Clinical Diagnostics, Tokyo, Japan).

SMase treatment. HCVcc was treated with SMase at various concentrations in DMEM for 1 h at 37°C and was then centrifuged at 100,000 × *g* for 3 h to form a pellet, which was resuspended in 0.5 ml of medium for the infection assays.

HCVcc binding and internalization assays. To monitor binding, cells grown in a 6-well plate were preincubated for 1 h at 4°C, after which B-CD- or SMase-treated HCVcc was bound to the cells for 1 h at 4°C. As a measure of virus internalization, following the virus binding procedure, the cells were warmed to 37°C and maintained for 2 h, after which they were treated with 0.25% trypsin for 10 min at 37°C. Huh7-25, a CD81-negative Huh-7 subclone (3), was used to ensure removal of surface-bound virus by trypsin treatment. For both the binding and internalization assays, the resulting cells, as described above, were washed with ice-cold phosphate-buffered saline, followed by lysis with TRIzol reagent (Invitrogen). Cell-associated virus was quantified by measuring the amount of HCV RNA in the cell lysate by the real-time reverse transcription-PCR method (2, 34). Cells were treated with heparinase as previously described (33).

HCV replication assay in HCVcc-infected or replicon cells. HCV subgenomic replicon cells or cells infected with HCVcc were treated with various concentrations of inhibitors for 72 h. Total RNA was isolated from replicon cells using TRIzol reagent (Invitrogen), followed by quantification of HCV RNA by real-time reverse transcription-PCR as previously described (2, 34). Levels of core protein in the culture supernatants of HCVcc-infected cells were tested as described above.

Detection of cholesterol content of HCVcc. For [^{3}H]cholesterol labeling of viruses, HCVcc-infected or uninfected cells were incubated with 50 mCi of [1α,2α-^{3}H]cholesterol in DMEM for 24 h. Culture supernatants of the cells were incubated in the presence or absence of B-CD at 5 mg/ml for 1 h at 37°C, followed by ultracentrifugation on a 60% sucrose cushion. The virus-containing fractions and corresponding fractions from an uninfected culture were lysed in the buffer containing 1% Triton X-100 (TX-100), and radioactivity was quantified by scintillation counting. Radioactivities (in counts per minute) of HCVcc samples were determined by subtracting the radioactivity of uninfected cells from that of HCVcc-infected cells.

TABLE 1. Cholesterol and phospholipid contents of HCVcc and cells

Cell type or virus	Content (nmol/mg of protein)[a]		Chol/PL ratio
	Chol	PL	
Cells			
Uninfected	105.9 ± 10.4	253.2 ± 10.6	0.42
JFH-1 infected	116.5 ± 10.0	292.0 ± 18.4	0.40
Virus			
JFH-1	43.6 ± 2.4	33.8 ± 1.8	1.29
J6/JFH-1[b]	28.7 ± 4.8	22.7 ± 2.9	1.26

[a] Data are averages of three independent measurements ± standard deviations. Chol, cholesterol; PL, phospholipids.

[b] J6/JFH1 virus was produced from the pJ6/N2X-JFH1 construct and has structural proteins from the J6CF strain.

Metabolic labeling analysis of sphingolipid content. After 2 h of incubation with [^{14}C]serine (0.5 mCi/ml) in Opti-MEM (Invitrogen), the cells were lysed with 0.1% sodium dodecyl sulfate, and total lipid was extracted with chloroform-methanol (1:2, vol/vol). The extracts were spotted onto silica gel 60 plates (Merck, Darmstadt, Germany) and chromatographed with methyl acetate–1-propanol–chloroform–methanol–0.25% KCl (25:25:25:10:9, vol/vol). Radioactive spots were quantitatively detected by BAS 2000 (Fuji Film, Japan).

Membrane flotation assay. The membrane flotation assay was performed as previously described (46).

RESULTS

Critical role of virion-associated cholesterol. A role of virion-associated cholesterol in infectivity has been demonstrated for several enveloped viruses (4). However, little is known about the role of lipids associated with the virions of flaviviruses, including HCV, and their contribution to the viral life cycle. To determine the lipid composition of mature HCV virions, we extracted total lipid from HCVcc (JFH-1 and chimeric J6/JFH-1) prepared from the culture supernatants of cells infected with HCV, as well as the total cellular membrane fractions of uninfected and infected Huh-7 cells. The cholesterol and phospholipid contents were quantified, because these are the two major lipid constituents of biological membranes. The cholesterol-to-phospholipid molar ratio, which is known as a parameter of membrane viscosity (47), was significantly higher in virus samples (1.29 and 1.26 for JFH-1 and J6/JFH-1, respectively) than in cell membrane samples (0.40 and 0.42 for JFH-1-infected and uninfected cells, respectively) (Table 1). The ratios in viral samples were similar to or greater than those in mammalian plasma membranes, where most cellular cholesterol is found. Minimal contamination of the viral samples with extracellular microvesicles likely occurred, since only a small amount of lipid was detected in a sample prepared from the culture medium of uninfected cells (data not shown). Thus, it is likely that HCV virions are enriched with cholesterol during assembly and maturation.

To investigate a potential role for the particular lipid composition of HCV particles, HCVcc was treated with

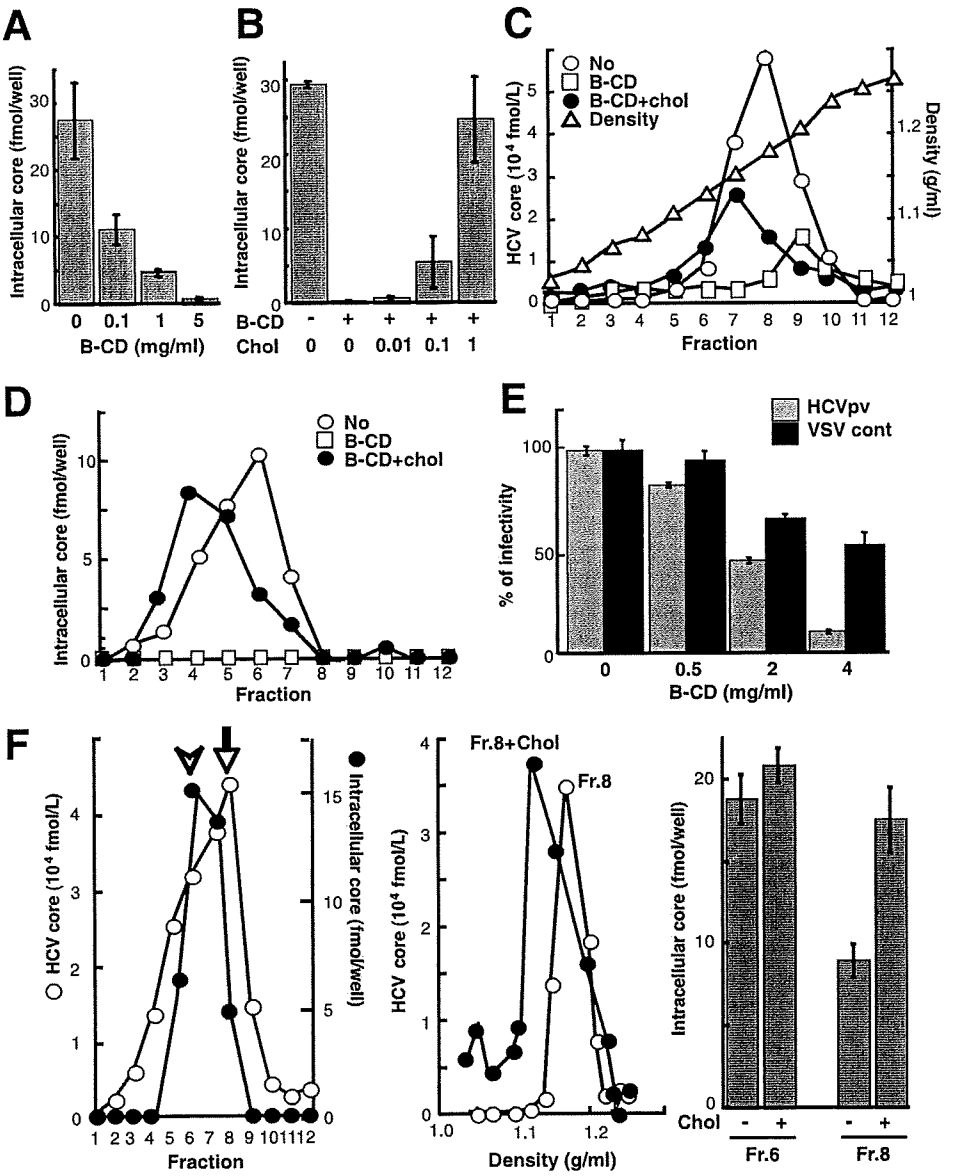

FIG. 1. Role of HCV-associated cholesterol in infection. (A) Effect of cholesterol depletion on HCV infectivity. HCVcc particles (~2 fmol of the core protein) were treated with B-CD at 0.1, 1, and 5 mg/ml for 1 h at 37°C. After removal of B-CD, Huh-7 cells were infected with the treated virus particles, after which the core protein content of infected cells at 72 h p.i. was determined as an indicator of infectivity, as previously established (24). (B) Effect of cholesterol replenishment on infectivity. After treatment with 5 mg/ml B-CD, virus was treated either with medium alone or with medium containing exogenous cholesterol for 1 h at 37°C. (C) Effect of cholesterol depletion and replenishment on density gradient profiles of the viral particles. The HCVcc treated with 5 mg/ml B-CD was replenished with exogenous cholesterol (1 mM) and then separated by 10-to-60% sucrose gradient ultracentrifugation. The core protein in each fraction was measured. The density of each fraction was determined by refractive index measurement. (D) Effects of cholesterol depletion and replenishment on viral infectivity. Each fraction (see panel C) was infected, and then the core proteins in the cells were measured at 72 h p.i. (E) Effect of cholesterol depletion on the infectivity of HCVpv (genotype 1a) (shaded bars) or the control, VSVdelG-GFP/G (solid bars). The viruses were preincubated with B-CD for 1 h at 37°C before infection. (F) (Left) The culture medium from HCVcc-producing cells was fractionated as described above. For each fraction, the amounts of core and intracellular core (infectivity) are plotted. Peaks of the core (arrow) and infectivity (arrowhead) are indicated. (Center) An aliquot of fraction 8 (peak of the core) was treated with 1 mM cholesterol for 1 h at 37°C. The resultant aliquot and an untreated aliquot of the fraction were subjected to sucrose gradient ultracentrifugation. The core in each fraction was plotted. (Right) The infectivities of fractions (Fr.) 6 and 8 (see the left panel) with or without cholesterol treatment were determined as shown above. Data are means from four independent experiments. Error bars, standard deviations.

increasing concentrations (0.1 to 5 mg/ml) of B-CD, which is known to extract cholesterol from membranes (40). The viral samples were then used to inoculate Huh-7 cells after removal of B-CD by ultracentrifugation. Infectivity was evaluated by quantifying the viral core protein in cells at 72 h postinfection (p.i.). Using an immunoassay that provides results indicative of HCV infectivity (25), we also confirmed a good correlation between the core level and

TABLE 2. Depletion of virion-associated cholesterol by B-CD

Treatment	Radioactivity (cpm) of HCVcc[a]		Avg (%[b])
	Expt 1	Expt 2	
None	5,327	5,573	5,450 (100)
B-CD (5 mg/ml)	3,643	1,646	2,644 (48.5)

[a] Determined by subtracting the radioactivity of uninfected cells from that of HCVcc-infected cells in two experiments.
[b] Percentage of the radioactivity of the untreated sample.

infectious titers (data not shown). As shown in Fig. 1A, core protein levels following B-CD treatment at 0.1, 1, or 5 mg/ml were reduced by 60, 83, or 98%, respectively, from the levels with the untreated virus. The cholesterol level of HCVcc treated with 5 mg/ml B-CD was found to be ~50% of that of untreated virions (Table 2).

To demonstrate that the reduced infection efficiency of B-CD-treated virus was caused by the reduced cholesterol content of the viral envelope, we attempted to reverse the inhibitory effect by adding exogenous cholesterol. Following treatment of HCVcc with 5 mg/ml B-CD, the drug was washed out, and increasing concentrations of cholesterol were added in an attempt to reconstitute the normal virion cholesterol content. The addition of 1 mM cholesterol completely reversed the virus infectivity (Fig. 1B). After cholesterol was replenished, the viral RNA was restored to a level similar to that in the untreated control.

To investigate the effect of cholesterol on the density of infectious HCV virions, B-CD-pretreated or untreated viral samples, as well as cholesterol-replenished treated viral samples, were subjected to sucrose density gradient centrifugation (Fig. 1C). The density of HCVcc core protein at its peak concentration in untreated virus samples was ~1.17 g/ml. When virion-associated cholesterol was removed by B-CD, the density of HCVcc core protein at its peak concentration was shifted to 1.20 g/ml. Addition of exogenous cholesterol to this cholesterol-depleted sample restored a lower-density fraction (1.15 g/ml). Figure 1D illustrates the infectivity of each gradient fraction. Untreated virus had maximum infectivity at ~1.13 g/ml (fraction 6), while, as expected, fractions from B-CD-treated viral samples exhibited minimal to no infectivity. Replenishment of depleted virus with cholesterol returned infectivity to untreated-control levels, and cholesterol-replenished virus had a buoyant density of ~1.07 g/ml (fraction 4), suggesting that HCV-associated cholesterol is crucial for viral infectivity and that the effect of a cholesterol-depleting drug is reversible. We further observed that B-CD treatment of a pseudotyped VSV containing the E1 and E2 proteins of the HCV genotype 1a isolate H77c (HCVpv) resulted in a progressive loss of infectivity, while B-CD had significantly less impact on the infectivity of the control virus VSVdelG-GFP/G (Fig. 1E).

The results described above raise the possibility that the infectivity of HCV virions with relatively low levels of incorporated cholesterol might be enhanced by supplementation with exogenous cholesterol. Density gradient fractions of culture supernatants collected from HCV-infected cells were analyzed with regard to the presence of core protein and infectivity (Fig. 1F, left). As indicated above, maximum infectivity was obtained with fraction 6 (1.13 g/ml). In contrast, a major fraction of core protein banded at a higher density (1.17 g/ml) in fraction 8. We hypothesized that fraction 8 contains lipids at lower levels than those in fraction 6. However, quantification of lipids, including cholesterol, in the fractions obtained failed, presumably due to a low sensitivity of detection. Thus, to extend our findings on the involvement of cholesterol, we added exogenous cholesterol to fraction 8, followed by ultrafiltration to remove unincorporated cholesterol. A subsequent density gradient profile demonstrated a shift in the core protein peak to 1.13 g/ml (Fig. 1F, center). A concomitant increase in the infectivity of the fraction, approaching that of untreated fraction 6, was observed (Fig. 1F, right). In contrast, supplementation of fraction 6 with exogenous cholesterol did not alter its infectivity (Fig. 1F, right) or change its density gradient (data not shown). These results suggest that exogenous cholesterol supplementation can reverse deficits in the infectivity of HCV virions due to low cholesterol content.

Sphingolipid dependence of HCV infectivity. In addition to cholesterol, sphingolipid is a major component of eukaryotic lipid membranes. We therefore investigated the functional significance of sphingomyelin (SM), the most abundant sphingolipid, with regard to HCV infectivity. HCVcc was treated for 1 h with increasing concentrations (0.1 to 10 U/ml) of bacterial SMase, which is known to hydrolyze membrane-bound SM to ceramide. Following ultracentrifugation to remove the SMase, Huh-7 cells were inoculated with the HCVcc. The amount of HCV core protein within the cells was quantified at 72 h p.i. Figure 2A shows 50 and 90% reductions in HCV infectivity after incubation of the virion with 0.1 and 1 U/ml SMase, respectively. We further observed that SMase treatment of HCVpv resulted in a progressive loss of infectivity, while SMase had no effect on the infectivity of the control virus (Fig. 2B). This demonstrates that sphingolipid, like cholesterol, plays an essential role in HCV infectivity.

Requirement for virion-associated cholesterol and sphingolipid during HCV cell entry. These findings support the idea that virion-associated cholesterol and sphingolipid may influence viral entry into host cells by altering the interaction between viral particles and a host cell factor(s). Viral entry is a multistep process including binding of the virion to the cell surface and internalization into the cytoplasm by endocytosis. To examine whether virion-associated cholesterol and SM might play a role in cell binding or postbinding events during viral entry, we used a binding assay in which Huh-7 cells preincubated for 1 h at 4°C were infected with B-CD- or SMase-treated HCVcc. Total RNA was extracted after a 1-h addition of the virions at 4°C, followed by quantification of HCV RNA. As shown in Fig. 3A, treatment of the virions with either B-CD or SMase had little influence on their ability to bind to cells.

It has been shown that CD81 plays an important role in HCV internalization but is not correlated with viral attachment (7, 33). An anti-CD81 antibody was used as a negative control for reduced viral attachment. It is likely that heparan sulfate proteoglycan on the target cell surface is needed for the initial attachment of HCV (33). Thus, heparinase I was used as a positive control for reduced HCV attachment to the cells. To examine the roles of cholesterol and sphingolipid on the HCVcc membrane in viral internalization, a virus-cell mixture

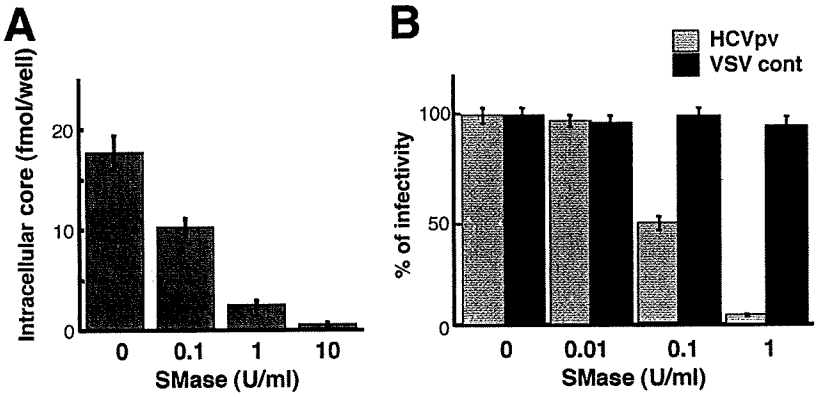

FIG. 2. Effect of SM hydrolysis on viral infectivity. (A) Effect on the infectivity of HCVcc. HCVcc was treated with 0.1, 1, or 10 U/ml SMase for 1 h at 37°C, after which SMase was removed by ultracentifugation. Huh-7 cells were infected with the treated virus, and the core protein content of infected cells was determined at 72 h p.i. (B) Effect on the infectivity of HCVpv (genotype 1a) (shaded bars) or the control, VSVdelG-GFP/G (VSV cont) (solid bars). The viruses were preincubated with SMase for 1 h at 37°C before infection. Data are means from four independent experiments. Error bars, standard deviations.

prepared at 4°C as described above was incubated for 2 h at 37°C, followed by trypsinization to remove virions that were surface bound but not internalized (Fig. 3B). We verified that 94% of surface-bound-viruses were removed by trypsinization using CD81-negative Huh-7 subclones. A marked reduction in viral RNA levels within cells was detected after pretreatment of the virus with either B-CD or SMase. These results strongly suggest that virion-associated cholesterol and sphingolipid function as key determinants of internalization but not of cell attachment.

Association of HCV structural proteins with lipid rafts. Cholesterol and sphingolipid are major components of lipid rafts, which can be isolated as detergent-resistant membranes (DRMs) by treatment with cold TX-100, followed by equilibrium flotation centrifugation. Matto et al. (30) reported that HCV core protein is associated with DRMs in cells carrying the full-length HCV replicon. To investigate whether HCV structural proteins are associated with DRMs in HCVcc-producing cells, lysates from cells infected with HCVcc were subjected to membrane flotation analysis. In the absence of detergent treatment, the majority of the core (Fig. 4A) and E1 (Fig. 4B) proteins were detected in the membrane fractions. After treatment with cold TX-100, significant amounts of both viral proteins were recovered from the DRM fraction. However, after treatment with TX-100 at 37°C, the majority of the E1 and core proteins had shifted to the detergent-soluble fractions. We also found that HCV genotype 1b E1 and E2 can be associated with the lipid raft in 293T cells transfected with an E1 or E2 expression plasmid (Fig. 4C) and that the cytoplasmic tails of envelope

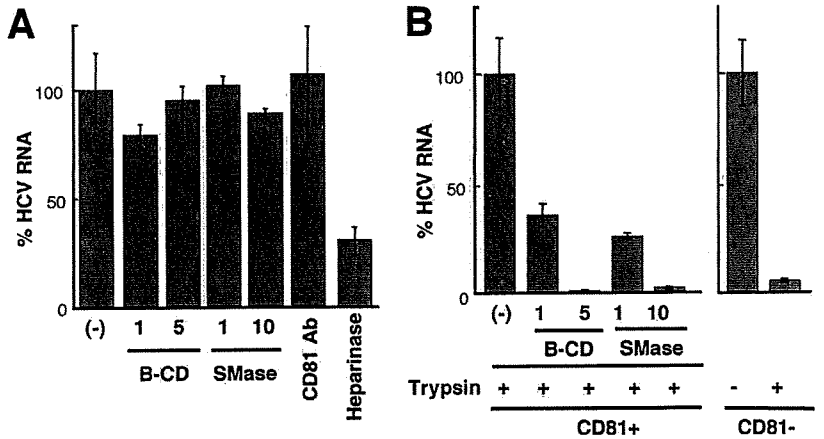

FIG. 3. Effects of B-CD or SMase on virus attachment and internalization. (A) Virus attachment to Huh-7 cells was determined at 4°C after treatment of HCVcc with B-CD (1 or 5 mg/ml) or SMase (1 or 10 U/ml). An antibody (Ab) against CD81 was used, in order to ensure that the antibody did not inhibit HCVcc binding (7, 33). Heparinase was used to reduce HCV attachment to the cell. Viral RNA copies were normalized to total cellular RNA, and the normalized RNA copies in the mock-treated sample (−) were arbitrarily set at 100%. (B) Virus internalization was measured in Huh7-25, a CD81-negative subclone ($CD81^-$) (3), and Huh7-25-CD81, which stably expresses CD81 ($CD81^+$), after treatment of the virions with B-CD or SMase. After internalization for 2 h at 37°C, cells were exposed to trypsin (trypsin +) or phosphate-buffered saline (trypsin −). Huh7-25 was used to ensure that surface-bound virus would be removed by trypsin treatment. The amounts of HCV RNA in Huh7-25 and Huh7-25-CD81 cells infected with untreated HCVcc were assigned the arbitrary value of 100%, respectively. Results are representative of four independent experiments.

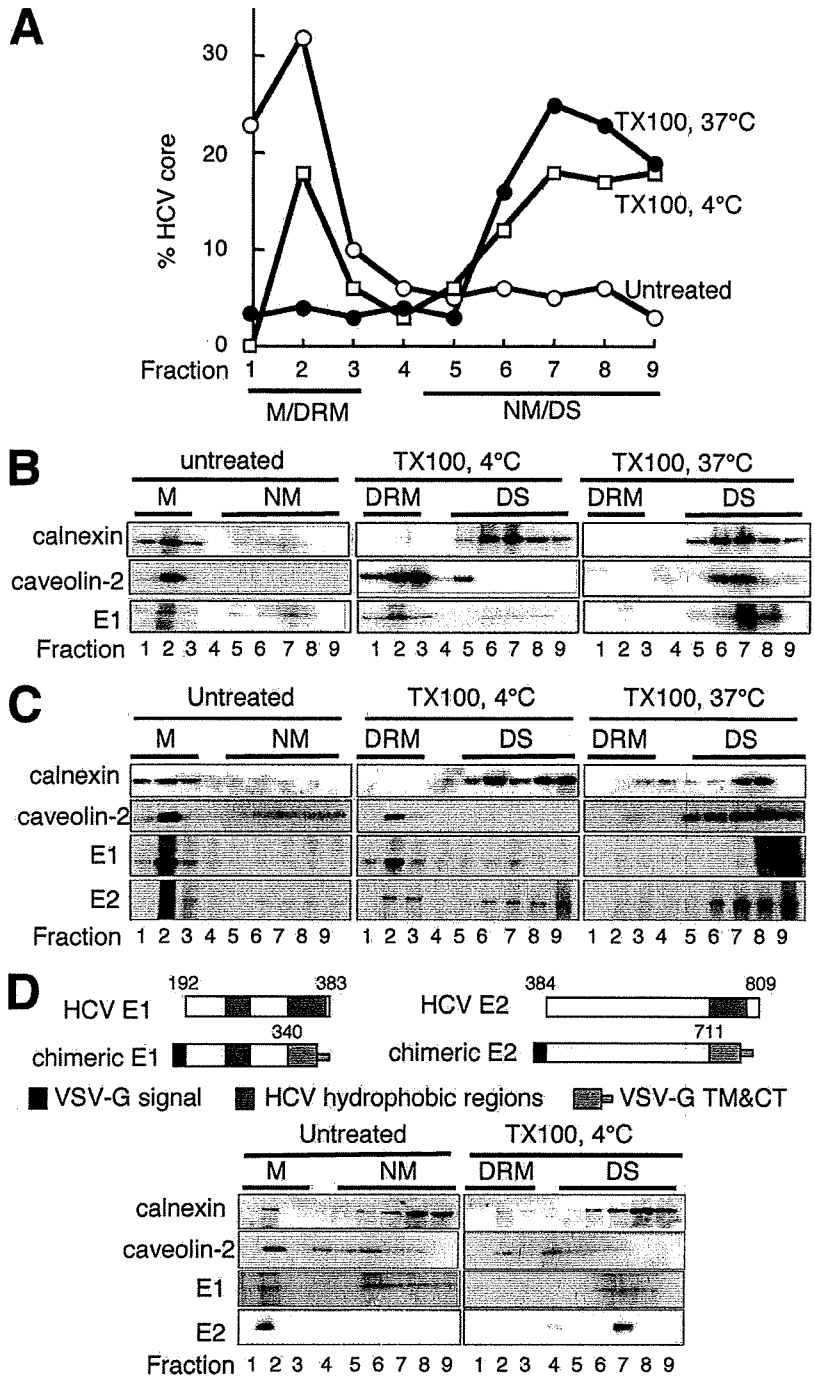

FIG. 4. Compartmentation of HCV structural proteins within DRM fractions. Lysates of HCVcc-infected cells were either treated with 1% TX-100, either on ice or at 37°C, or left untreated, followed by sucrose gradient centrifugation. (A and B) For each fraction, the amount of core protein was determined by an enzyme-linked immunosorbent assay (A), and E1, calnexin, and caveolin-2 were analyzed by Western blotting (B). The amount of core protein in each lysate (TX-100, 37°C; TX-100, 4°C; Untreated) was assigned the arbitrary value of 100%. M, membrane; NM, nonmembrane; DS, detergent soluble. (C) Lysates of 293T cells expressing HCV E1 or E2 protein were either treated with 1% TX-100, either on ice or at 37°C, or left untreated, followed by discontinuous sucrose gradient centrifugation. Each fraction was concentrated in a Centricon YM-30 filter unit and subjected to 12.5% sodium dodecyl sulfate-polyacrylamide gel electrophoresis, followed by immunoblotting with antibodies against calnexin, caveolin-2, Myc (E1), or FLAG (E2). (D) (Top) Structures of HCV envelope genes used. Amino acid positions of HCV are indicated. Signal sequence, transmembrane (TM), and cytoplasmic tail (CT) domains of VSV G protein are shown. (Bottom) Cell lysates expressing chimeric HCV E1 or E2 protein were treated with 1% TX-100 on ice or left untreated, followed by discontinuous sucrose gradient centrifugation. It has been reported that VSV-G is not associated with lipid (39). Calnexin, caveolin-2, and chimeric glycoproteins (chimeric E1 and chimeric E2) were analyzed by immunoblotting. Fractions are numbered from 1 to 9 in order from top to bottom (light to heavy).

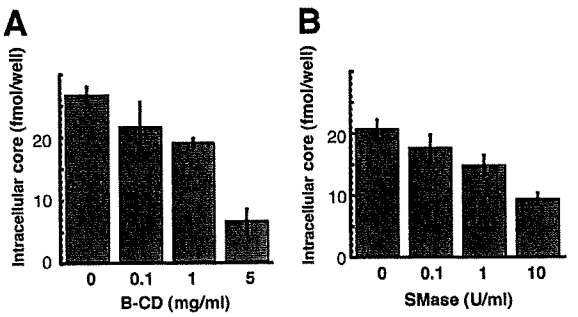

FIG. 5. Effects of B-CD or SMase treatment of cells on HCV infectivity. Huh-7 cells were either left untreated or treated with B-CD at 0.1, 1, or 5 mg/ml (A) or with SMase at 0.1, 1, or 10 U/ml (B) prior to HCVcc infection. Intracellular core levels were quantitated 72 h p.i. Data are means from four independent experiments. Error bars, standard deviations.

proteins are important for their interaction (Fig. 4D). These data suggest that subpopulations of HCV structural proteins are associated with lipid rafts in cells generating the HCV particles.

Moderate inhibition of HCV infection by B-CD or SMase treatment of host cells. It has recently been reported that cholesterol depletion or SM hydrolysis from the host cell membrane decreases HCV infection, in part by decreasing the level of CD81 on the cell surface (19, 53). The involvement of the lipid environment of the host cell plasma membrane in HCV infection was investigated in our HCVcc infection system. Prior to infection, Huh-7 cells were treated with B-CD or SMase and then washed with the medium five times. Cholesterol depletion from Huh-7 cells by B-CD at 1 or 5 mg/ml inhibited HCV core levels by 20 and 75%, respectively, compared to levels in untreated cells (Fig. 5A). We also found that hydrolysis of SM by SMase at 1 or 10 U/ml on the cells, respectively, led to moderate reduction of the viral infection, by 20 or 55% of the infection level of the untreated control (Fig. 5B). There was no influence on cell viability under the conditions of these treatments (data not shown). These findings, compared with the results in Fig. 1A and 2A, suggest that the raft-like environment on the plasma membrane likely serves as a portal for HCV entry, but HCV virion-associated cholesterol and sphingolipid more readily play more critical roles in viral infection.

Inhibitors of the sphingolipid biosynthetic pathway suppress the production of HCVcc, but not RNA replication, for a JFH-1-derived replicon. In the course of studying the involvement of lipid metabolism in the HCV life cycle, we observed that inhibitors of the sphingolipid biosynthetic pathway, including ISP-1 and HPA-12, which specifically inhibit serine palmitoyltransferase (31) and ceramide trafficking from the ER to the Golgi apparatus (55), influenced subgenomic replicons derived from the HCV-N isolate (genotype 1b), but not those derived from JFH-1. A dose-dependent decrease in HCV RNA copy numbers among HCV-N replicon cells was observed upon exposure to ISP-1 or HPA-12, as previously reported (43, 52). In contrast, these compounds had little or no effect on viral RNA accumulation in JFH-1 replicon cells (Fig. 6A). Furthermore, these compounds did not affect luciferase activity in the lysates of Huh-7 cells transfected with an in vitro-transcribed JFH-1 replicon RNA containing a luciferase reporter gene (22) (data not shown). Figure 6B shows the effects of ISP-1 and HPA-12 on de novo sphingolipid biosynthesis by replicon cells. No differences in the inhibitory effects of each compound were observed in replicon cells derived from HCV-N versus JFH-1. When de novo synthesis of sphingolipids was examined by metabolic labeling with [^{14}C]serine, ISP-1 almost completely inhibited the production of both ceramide and SM, while HPA-12 greatly inhibited the synthesis of SM but not ceramide. Levels of phosphatidylethanolamine and phosphatidylserine, into which serine is incorporated by a pathway distinct from that of sphingolipid biosynthesis, were not influenced by these drugs. These results suggest that suppression of HCV RNA replication by inhibitors of sphingolipid biosynthesis might be dependent on the viral genotype or isolate.

This observation prompted us to investigate whether inhibitors of the sphingolipid biosynthetic pathway might have the ability to prevent HCV virion production. Interestingly, when Huh-7 cells producing JFH-1 HCVcc were treated with ISP-1 or HPA-12 under conditions similar to those the replicon cells, viral core levels in the culture supernatants were greatly reduced in a dose-dependent manner. For example, exposure to 10 μM ISP-1 or 1 μM HPA-12 reduced viral core protein levels more than 85% from those for control cells (Fig. 6C). The 50% inhibitory concentrations of both drugs were less than 0.1 μM, 50-fold less than those obtained for the RNA replication of the HCV-N-replicon. Together, these results suggest that the sphingolipid biosynthetic pathway plays an important role in the production of HCV particles, but not in genome replication, in JFH-1-based HCVcc.

DISCUSSION

In this study, we demonstrated the role of HCV virion-associated cholesterol and sphingolipid in viral infectivity. Although dependence on virion-associated cholesterol for virus entry has been shown for a number of viruses (4, 6, 28, 49), this is the first study to demonstrate the importance of envelope cholesterol in a virus belonging to the family *Flaviviridae*. Furthermore, to our knowledge, the functional role of virion membrane-associated SM has not been examined in viruses. Our previous studies using Chinese hamster ovary cell mutants deficient in SM synthesis have demonstrated that reduction of cellular SM levels enhances cellular cholesterol efflux in the presence of B-CD (9, 12). Thus, it may be possible that SM plays a role in the retention of cholesterol on HCV particles due to interaction between cholesterol and SM. The finding that B-CD or SMase treatment of HCVcc markedly inhibited virus internalization but not cell attachment (Fig. 3) suggests that HCV membrane-associated cholesterol and sphingolipid are crucial for the interaction of viral glycoproteins with the virus-receptor/coreceptor required for cell entry. Cholesterol depletion or sphingolipid hydrolysis might induce a conformational change in the viral envelope, resulting in instability of the virion structure. Since the cholesterol/phospholipid ratios of membranes affect bilayer fluidity, the maturation of viral envelopes with high cholesterol/phospholipid ratios via association with rafts may be important for the stability of HCV

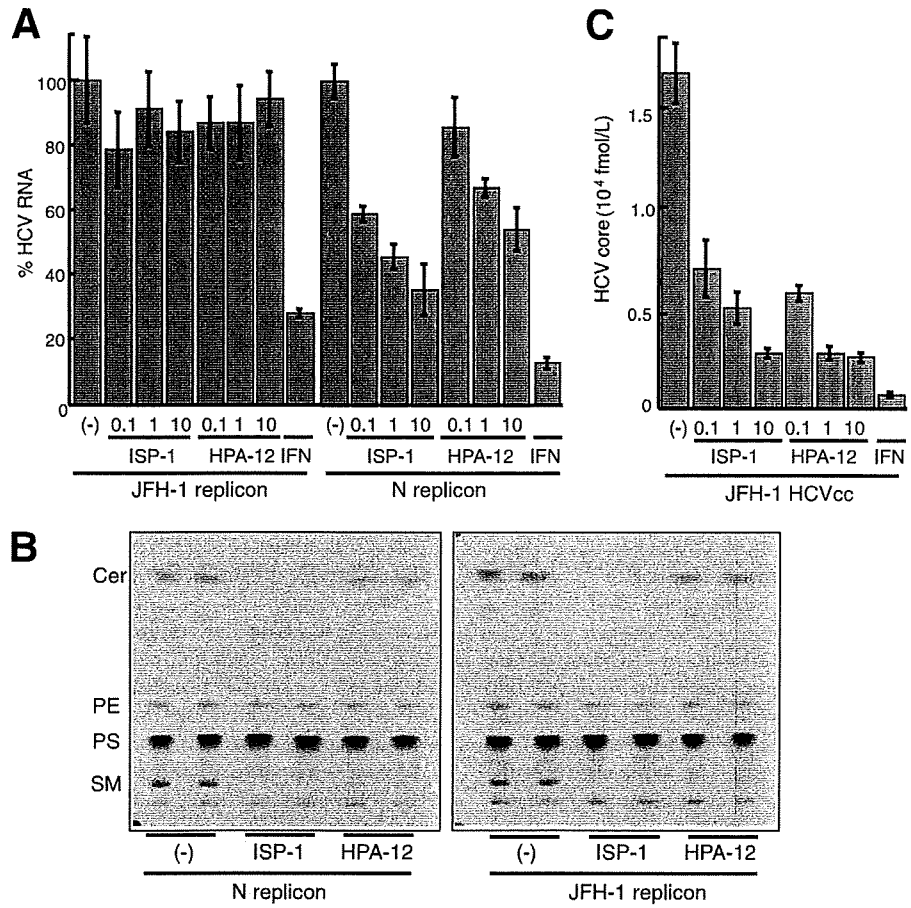

FIG. 6. Anti-HCV effects of inhibitors of the sphingolipid biosynthetic pathway. Subgenomic replicon cells derived from HCV isolate N or JFH-1, as well as HCVcc-producing cells, were treated with ISP-1 (0.1, 1, or 10 μM), HPA-12 (0.1, 1, or 10 μM) or alpha interferon (IFN) (100 U/ml) for 72 h. HCV RNA titers in the replicon cells (A) and the HCV core protein content of the culture medium of infected cells (C) were determined. Data are means from four independent experiments. Error bars, standard deviations. (B) De novo synthesis of sphingolipid in the absence or presence of ISP-1 (10 μM) and HPA-12 (10 μM) was monitored in duplicate by metabolic labeling with [^{14}C]serine for 2 h at 37°C. Cer, ceramide; PE, phosphatidylethanolamine; PS, phosphatidylserine.

particles. Replenishing the viral membrane with cholesterol following treatment with 5 mg/ml B-CD successfully restored viral infectivity to the same level as that of untreated virus (Fig. 1), suggesting that reversible B-CD-induced changes in HCV structure might critically influence viral infectivity. However, we were unable to restore viral infectivity by replenishing cholesterol after pretreatment of the virion with concentrations of B-CD exceeding 10 mg/ml (data not shown). Under these conditions, it is likely that large holes in the viral membrane destroy the virus, a result that cannot be reversed by supplying exogenous cholesterol.

How are cholesterol and sphingolipid involved in the HCV virion during the process of virus maturation? Like most positive-stranded RNA viruses, HCV is thought to assemble at the ER membrane. However, Miyanari et al. (32) reported that lipid droplets are important for HCVcc formation. These authors have shown that the characteristics of lipid-droplet-associated membranes in Huh-7 cells differ from those of ER membranes. In the case of flaviviruses, for which the mechanism of viral assembly and budding remains unclear (15), a few studies have demonstrated budding at the plasma membrane (13, 36, 37, 41), and it has been proposed that the site of budding may be virus and cell type dependent (27). We demonstrate here that subpopulations of HCV structural proteins partition into cellular detergent-resistant, lipid-raft-like membrane fractions in HCVcc-producing cells (Fig. 4) and that inhibitors of the sphingolipid biosynthetic pathway block HCV virion production (Fig. 6). Furthermore, a large proportion of HCV E2 protein incorporated into HCVcc is endoglycosidase H resistant (data not shown). Thus, membrane compartments containing cholesterol- and sphingolipid-rich microdomains may be involved in HCV virion maturation. Another explanation for the recruitment of these lipids to the HCV membrane may be an association between the virus and very-low-density lipoprotein (VLDL) or low-density lipoprotein. Recently, Huang et al. (16) demonstrated a close link between HCV production and VLDL assembly, suggesting that an HCV-VLDL complex is generated and secreted from cells.

Recent reports have demonstrated that CD81-mediated HCV infection is partly dependent on cell membrane choles-

terol (19) and SM (53). We further characterized the role of lipid on the plasma membrane in viral infectivity and found that cholesterol depletion by B-CD, as well as hydrolysis of SM by SMase, moderately inhibits HCV infectivity (Fig. 5). These results suggest that cholesterol and sphingolipid in the plasma membrane environment may assist HCV entry, while HCV virion-associated cholesterol and sphingolipid appear to play critical roles in viral infection.

We previously demonstrated that HCV RNA and nonstructural proteins are present in DRM structures, likely in the context of a lipid-raft structure, and that viral RNA is likely synthesized at a raft membrane structure in cells containing the genotype 1b HCV replicon (2, 10, 46). Here we observed that ISP-1 and HPA-12 suppress HCVcc production, but not viral RNA replication, by the JFH-1 replicon (Fig. 6). Impairment of particle assembly and maturation, rather than suppression of genome replication, by these drugs may account for the inhibition of HCV production in the JFH-1 system. Viral RNA replication of the HCV-N replicon, however, was efficiently inhibited by these compounds, as found in previous reports (43). The virus strain specificity of the anti-HCV activity of cyclosporine has recently been demonstrated: JFH-1 replication is less sensitive to cyclosporine than replication of genotype 1b strains. Furthermore, the requirement for interaction with a cellular replication cofactor, cyclophilin B, differs among HCV strains (18). It appears that ISP-1 and HPA-12 are further examples of diverse effects on HCV strain replication.

In summary, our data here demonstrate important roles of cholesterol and sphingolipid in HCV infection and virion maturation. Specifically, mature HCV particles are rich in cholesterol. Depletion from HCV or hydrolysis of virion-associated SM results in a loss of infectivity. Moreover, the addition of exogenous cholesterol restores infectivity. In addition, cholesterol and sphingolipid on the HCV membrane play key roles in virus internalization, and portions of structural proteins are localized at lipid-raft-like membrane structures within cells. Finally, inhibitors of the sphingolipid biosynthetic pathway efficiently block virion production. These observations suggest that agents capable of modifying virion-associated lipid content might function as antivirals by preventing and/or blocking HCV infection and production.

ACKNOWLEDGMENTS

We thank M. Matsuda, M. Sasaki, S. Yoshizaki, T. Shimoji, M. Kaga, and T. Date for technical assistance and T. Mizoguchi for secretarial work.

This work was partially supported by a grant-in-aid for Scientific Research from the Japan Society for the Promotion of Science, from the Ministry of Health, Labor, and Welfare of Japan, and from the Ministry of Education, Culture, Sports, Science, and Technology, as well as by a Research on Health Science Focusing on Drug Innovation grant from the Japan Health Sciences Foundation.

REFERENCES

1. **Aizaki, H., Y. Aoki, T. Harada, K. Ishii, T. Suzuki, S. Nagamori, G. Toda, Y. Matsuura, and T. Miyamura.** 1998. Full-length complementary DNA of hepatitis C virus genome from an infectious blood sample. Hepatology **27:** 621–627.
2. **Aizaki, H., K. J. Lee, V. M. Sung, H. Ishiko, and M. M. Lai.** 2004. Characterization of the hepatitis C virus RNA replication complex associated with lipid rafts. Virology **324:**450–461.
3. **Akazawa, D., T. Date, K. Morikawa, A. Murayama, M. Miyamoto, M. Kaga, H. Barth, T. F. Baumert, J. Dubuisson, and T. Wakita.** 2007. CD81 expression is important for the permissiveness of Huh7 cell clones for heterogeneous hepatitis C virus infection. J. Virol. **81:**5036–5045.
4. **Bender, F. C., J. C. Whitbeck, H. Lou, G. H. Cohen, and R. J. Eisenberg.** 2005. Herpes simplex virus glycoprotein B binds to cell surfaces independently of heparan sulfate and blocks virus entry. J. Virol. **79:**11588–11597.
5. **Blanchard, E., D. Brand, S. Trassard, A. Goudeau, and P. Roingeard.** 2002. Hepatitis C virus-like particle morphogenesis. J. Virol. **76:**4073–4079.
6. **Chazal, N., and D. Gerlier.** 2003. Virus entry, assembly, budding, and membrane rafts. Microbiol. Mol. Biol. Rev. **67:**226–237.
7. **Evans, M. J., T. von Hahn, D. M. Tscherne, A. J. Syder, M. Panis, B. Wolk, T. Hatziioannou, J. A. McKeating, P. D. Bieniasz, and C. M. Rice.** 2007. Claudin-1 is a hepatitis C virus co-receptor required for a late step in entry. Nature **446:**801–805.
8. **Ezelle, H. J., D. Markovic, and G. N. Barber.** 2002. Generation of hepatitis C virus-like particles by use of a recombinant vesicular stomatitis virus vector. J. Virol. **76:**12325–12334.
9. **Fukasawa, M., M. Nishijima, H. Itabe, T. Takano, and K. Hanada.** 2000. Reduction of sphingomyelin level without accumulation of ceramide in Chinese hamster ovary cells affects detergent-resistant membrane domains and enhances cellular cholesterol efflux to methyl-β-cyclodextrin. J. Biol. Chem. **275:**34028–34034.
10. **Gao, L., H. Aizaki, J. W. He, and M. M. Lai.** 2004. Interactions between viral nonstructural proteins and host protein hVAP-33 mediate the formation of hepatitis C virus RNA replication complex on lipid raft. J. Virol. **78:**3480–3488.
11. **Guo, J. T., V. V. Bichko, and C. Seeger.** 2001. Effect of alpha interferon on the hepatitis C virus replicon. J. Virol. **75:**8516–8523.
12. **Hanada, K., T. Hara, M. Fukasawa, A. Yamaji, M. Umeda, and M. Nishijima.** 1998. Mammalian cell mutants resistant to a sphingomyelin-directed cytolysin. Genetic and biochemical evidence for complex formation of the LCB1 protein with the LCB2 protein for serine palmitoyltransferase. J. Biol. Chem. **273:**33787–33794.
13. **Hase, T., P. L. Summers, K. H. Eckels, and W. B. Baze.** 1987. An electron and immunoelectron microscopic study of dengue-2 virus infection of cultured mosquito cells: maturation events. Arch. Virol. **92:**273–291.
14. **Heider, J. G., and R. L. Boyett.** 1978. The picomole determination of free and total cholesterol in cells in culture. J. Lipid Res. **19:**514–518.
15. **Heinz, F. X., and S. L. Allison.** 2003. Flavivirus structure and membrane fusion. Adv. Virus Res. **59:**63–97.
16. **Huang, H., F. Sun, D. M. Owen, W. Li, Y. Chen, M. Gale, and J. Ye.** 2007. Hepatitis C virus production by human hepatocytes dependent on assembly and secretion of very low-density lipoproteins. Proc. Natl. Acad. Sci. USA **104:**5848–5853.
17. **Ikeda, M., M. Yi, K. Li, and S. M. Lemon.** 2002. Selectable subgenomic and genome-length dicistronic RNAs derived from an infectious molecular clone of the HCV-N strain of hepatitis C virus replicate efficiently in cultured Huh7 cells. J. Virol. **76:**2997–3006.
18. **Ishii, N., K. Watashi, T. Hishiki, K. Goto, D. Inoue, M. Hijikata, T. Wakita, N. Kato, and K. Shimotohno.** 2006. Diverse effects of cyclosporine on hepatitis C virus strain replication. J. Virol. **80:**4510–4520.
19. **Kapadia, S. B., H. Barth, T. Baumert, J. A. McKeating, and F. V. Chisari.** 2007. Initiation of hepatitis C virus infection is dependent on cholesterol and cooperativity between CD81 and scavenger receptor B type I. J. Virol. **81:**374–383.
20. **Kato, T., A. Furusaka, M. Miyamoto, T. Date, K. Yasui, J. Hiramoto, K. Nagayama, T. Tanaka, and T. Wakita.** 2001. Sequence analysis of hepatitis C virus isolated from a fulminant hepatitis patient. J. Med. Virol. **64:**334–339.
21. **Kato, T., T. Date, M. Miyamoto, A. Furusaka, K. Tokushige, M. Mizokami, and T. Wakita.** 2003. Efficient replication of the genotype 2a hepatitis C virus subgenomic replicon. Gastroenterology **125:**1808–1817.
22. **Kato, T., T. Date, M. Miyamoto, M. Sugiyama, Y. Tanaka, E. Orito, T. Ohno, K. Sugihara, I. Hasegawa, K. Fujiwara, K. Ito, A. Ozasa, M. Mizokami, and T. Wakita.** 2005. Detection of anti-hepatitis C virus effects of interferon and ribavirin by a sensitive replicon system. J. Clin. Microbiol. **43:**5679–5684.
23. **Kato, T., T. Date, A. Murayama, K. Morikawa, D. Akazawa, and T. Wakita.** 2006. Cell culture and infection system for hepatitis C virus. Nat. Protoc. **1:**2334–2339.
24. **Kobayashi, S, K. Kakumoto, and M. Sugiura.** 2002. Transition metal salts-catalyzed aza-Michael reactions of enones with carbamates. Org. Lett. **18:** 1319–1322.
25. **Koutsoudakis, G., E. Herrmann, S. Kallis, R. Bartenschlager, and T. Pietschmann.** 2007. The level of CD81 cell surface expression is a key determinant for productive entry of hepatitis C virus into host cells. J. Virol. **81:**588–598.
26. **Lohmann, V., F. Korner, J. Koch, U. Herian, L. Theilmann, and R. Bartenschlager.** 1999. Replication of subgenomic hepatitis C virus RNAs in a hepatoma cell line. Science **285:**110–113.
27. **Mackenzie, J. M., and E. G. Westaway.** 2001. Assembly and maturation of the flavivirus Kunjin virus appear to occur in the rough endoplasmic reticulum and along the secretory pathway, respectively. J. Virol. **75:**10787–10799.
28. **Manes, S., G. del Real, R. A. Lacalle, P. Lucas, C. Gomez-Mouton, S. Sanchez-Palomino, R. Delgado, J. Alcami, E. Mira, and A. C. Martinez.**

2000. Membrane raft microdomains mediate lateral assemblies required for HIV-1 infection. EMBO 1:190–196.
29. **Matsuo, E., H. Tani, C. Lim, Y. Komoda, T. Okamoto, H. Miyamoto, K. Moriishi, S. Yagi, A. H. Patel, T. Miyamura, and Y. Matsuura.** 2006. Characterization of HCV-like particles produced in a human hepatoma cell line by a recombinant baculovirus. Biochem. Biophys. Res. Commun. **340**:200–208.
30. **Matto, M., C. M. Rice, B. Aroeti, and J. S. Glenn.** 2004. Hepatitis C virus core protein associates with detergent-resistant membranes distinct from classical plasma membrane rafts. J. Virol. **78**:12047–12053.
31. **Miyake, Y., Y. Kozutsumi, S. Nakamura, T. Fujita, and T. Kawasaki.** 1995. Serine palmitoyltransferase is the primary target of a sphingosine-like immunosuppressant, ISP-1/myriocin. Biochem. Biophys. Res. Commun. **211**: 396–403.
32. **Miyanari, Y., K. Atsuzawa, N. Usuda, K. Watashi, T. Hishiki, M. Zayas, R. Bartenschlager, T. Wakita, M. Hijikata, and K. Shimotohno.** 2007. The lipid droplet is an important organelle for hepatitis C virus production. Nat. Cell Biol. **9**:1089–1097.
33. **Morikawa, K., Z. Zhao, T. Date, M. Miyamoto, A. Murayama, D. Akazawa, J. Tanabe, S. Sone, and T. Wakita.** 2007. The roles of CD81 and glycosaminoglycans in the adsorption and uptake of infectious HCV particles. J. Med. Virol. **79**:714–723.
34. **Murakami, K., K. Ishii, Y. Ishihara, S. Yoshizaki, K. Tanaka, Y. Gotoh, H. Aizaki, M. Kohara, H. Yoshioka, Y. Mori, N. Manabe, I. Shoji, T. Sata, R. Bartenschlager, Y. Matsuura, T. Miyamura, and T. Suzuki.** 2006. Production of infectious hepatitis C virus particles in three-dimensional cultures of the cell line carrying the genome-length dicistronic viral RNA of genotype 1b. Virology **351**:381–392.
35. **Nakai, K., T. Okamoto, T. Kimura-Someya, K. Ishii, C. K. Lim, H. Tani, E. Matsuo, T. Abe, Y. Mori, T. Suzuki, T. Miyamura, J. H. Nunberg, K. Moriishi, and Y. Matsuura.** 2006. Oligomerization of hepatitis C virus core protein is crucial for interaction with the cytoplasmic domain of E1 envelope protein. J. Virol. **80**:11265–11273.
36. **Ng, M. L., J. Howe, V. Sreenivasan, and J. J. Mulders.** 1994. Flavivirus West Nile (Sarafend) egress at the plasma membrane. Arch. Virol. **137**:303–313.
37. **Ng, M. L., S. H. Tan, and J. J. Chu.** 2001. Transport and budding at two distinct sites of visible nucleocapsids of West Nile (Sarafend) virus. J. Med. Virol. **65**:758–764.
38. **Niwa, H., K. Yamamura, and J. Miyazaki.** 1991. Efficient selection for high-expression transfectants with a novel eukaryotic vector. Gene **108**:193–199.
39. **Pessin, J. E., and M. Glaser.** 1980. Budding of Rous sarcoma virus and vesicular stomatitis virus from localized lipid regions in the plasma membrane of chicken embryo fibroblasts. J. Biol. Chem. **255**:9044–9050.
40. **Pitha, J., T. Irie, P. B. Sklar, and J. S. Nye.** 1988. Drug solubilizers to aid pharmacologists: amorphous cyclodextrin derivatives. Life Sci. **43**:493–502.
41. **Rahman, S., T. Matsumura, K. Masuda, K. Kanemura, and T. Fukunaga.** 1998. Maturation site of dengue type 2 virus in cultured mosquito C6/36 cells and Vero cells. Kobe J. Med. Sci. **44**:65–79.
42. **Rouser, G., G. Galli, and G. Kritchevsky.** 1967. Lipid composition of the normal human brain and its variations during various diseases. Pathol. Biol. **15**:195–200.
43. **Sakamoto, H., K. Okamoto, M. Aoki, H. Kato, A. Katsume, A. Ohta, T. Tsukuda, N. Shimma, Y. Aoki, M. Arisawa, M. Kohara, and M. Sudoh.** 2005. Host sphingolipid biosynthesis as a target for hepatitis C virus therapy. Nat. Chem. Biol. **1**:333–337.
44. **Sato, K., H. Okamoto, S. Aihara, Y. Hoshi, T. Tanaka, and S. Mishiro.** 1993. Demonstration of sugar moiety on the surface of hepatitis C virions recovered from the circulation of infected humans. Virology **196**:354–357.
45. **Serafino, A., M. B. Valli, F. Andreola, A. Crema, G. Ravagnan, L. Bertolini, and G. Carloni.** 2003. Suggested role of the Golgi apparatus and endoplasmic reticulum for crucial sites of hepatitis C virus replication in human lymphoblastoid cells infected in vitro. J. Med. Virol. **70**:31–41.
46. **Shi, S. T., K. J. Lee, H. Aizaki, S. B. Hwang, and M. M. Lai.** 2003. Hepatitis C virus RNA replication occurs on a detergent-resistant membrane that cofractionates with caveolin-2. J. Virol. **77**:4160–4168.
47. **Shinitzky, M., and M. Inbar.** 1976. Microviscosity parameters and protein mobility in biological membranes. Biochim. Biophys. Acta **433**:133–149.
48. **Shirakura, M., K. Murakami, T. Ichimura, R. Suzuki, T. Shimoji, K. Fukuda, K. Abe, S. Sato, M. Fukasawa, Y. Yamakawa, M. Nishijima, K. Moriishi, Y. Matsuura, T. Wakita, T. Suzuki, P. M. Howley, T. Miyamura, and I. Shoji.** 2007. E6AP ubiquitin ligase mediates ubiquitylation and degradation of hepatitis C virus core protein. J. Virol. **81**:1174–1185.
49. **Stuart, A. D., H. E. Eustace, T. A. McKee, and T. D. Brown.** 2002. A novel cell entry pathway for a DAF-using human enterovirus is dependent on lipid rafts. J. Virol. **76**:9307–9322.
50. **Takikawa, S., K. Ishii, H. Aizaki, T. Suzuki, H. Asakura, Y. Matsuura, and T. Miyamura.** 2000. Cell fusion activity of hepatitis C virus envelope proteins. J. Virol. **74**:5066–5074.
51. **Tani, H., Y. Komoda, E. Matsuo, K. Suzuki, I. Hamamoto, T. Yamashita, K. Moriishi, K. Fujiyama, T. Kanto, N. Hayashi, A. Owsianka, A. H. Patel, M. A. Whitt, and Y. Matsuura.** 2007. Replication-competent recombinant vesicular stomatitis virus encoding hepatitis C virus envelope proteins. J. Virol. **81**:8601–8612.
52. **Umehara, T., M. Sudoh, F. Yasui, C. Matsuda, Y. Hayashi, K. Chayama, and M. Kohara.** 2006. Serine palmitoyltransferase inhibitor suppresses HCV replication in a mouse model. Biochem. Biophys. Res. Commun. **346**:67–73.
53. **Voisset, C., M. Lavie, F. Helle, A. Op De Beeck, A. Bilheu, J. Bertrand-Michel, F. Tercé, L. Cocquerel, C. Wychowski, N. Vu-Dac, and J. Dubuisson.** 2008. Ceramide enrichment of the plasma membrane induces CD81 internalization and inhibits hepatitis C virus entry. Cell. Microbiol. **10**:606–617.
54. **Wakita, T., T. Pietschmann, T. Kato, T. Date, M. Miyamoto, Z. Zhao, K. Murthy, A. Habermann, H. G. Krausslich, M. Mizokami, R. Bartenschlager, and T. J. Liang.** 2005. Production of infectious hepatitis C virus in tissue culture from a cloned viral genome. Nat. Med. **11**:791–796.
55. **Yasuda, S., H. Kitagawa, M. Ueno, H. Ishitani, M. Fukasawa, M. Nishijima, S. Kobayashi, and K. Hanada.** 2001. A novel inhibitor of ceramide trafficking from the endoplasmic reticulum to the site of sphingomyelin synthesis. J. Biol. Chem. **276**:43994–44002.
56. **Zhong, J., P. Gastaminza, G. Cheng, S. Kapadia, T. Kato, D. R. Burton, S. F. Wieland, S. L. Uprichard, T. Wakita, and F. V. Chisari.** 2005. Robust hepatitis C virus infection in vitro. Proc. Natl. Acad. Sci. USA **102**:9294–9299.

nature chemical biology

Diverse backbone-cyclized peptides via codon reprogramming

Takashi Kawakami[1,4], Atsushi Ohta[1,4], Masaki Ohuchi[2], Hiroshi Ashigai[1], Hiroshi Murakami[3] & Hiroaki Suga[1–3]

We report a methodology for the ribosomal synthesis of backbone-cyclized peptides involving genetic code reprogramming to introduce one or more nonproteinogenic amino acids. Expression of linear peptides bearing a cysteine-proline dipeptide sequence followed by glycolic acid results in self-rearrangement to a C-terminal diketopiperadine-thioester, which non-enzymatically generates a cyclized peptide. We demonstrate the ribosomal synthesis of several naturally occurring backbone-cyclized peptides and a library based on a bicyclic scaffold, and we identify bioactive sequences by screening and deconvolution.

One of the common backbone frameworks found in many naturally occurring short peptides is a cyclic structure that connects the N and C termini (**Fig. 1a**). Even though such cyclic peptides are initially synthesized as linear peptides by ribosomes[1] or nonribosomal peptide synthetases[2], the enzymatic cyclization of the precursor linear peptides at the N and C termini grants them unique biological properties that their precursor peptides do not have, such as proteolytic stability[3] and high affinity toward their binding partners or targets[4]. This study reports a new enabling methodology that generates backbone-cyclized peptides amenable to the multiple introduction of non-natural amino acids in a reconstituted translation system.

A recent study reported the solid-phase synthesis of peptides containing a Cys-Pro-glycolic acid (^{HO}G) sequence in which these residues self-rearrange to form a diketopiperadine-thioester (dkp-thioester) derived from the conjugation of cysteine and proline via the non-enzymatic nitrogen to sulfur equilibrium shift driven by the concomitant release of the ^{HO}G residue[5]. The resultant thioester was then used to ligate two peptide fragments together. We envisioned that this elegant strategy could also be applied to peptide backbone

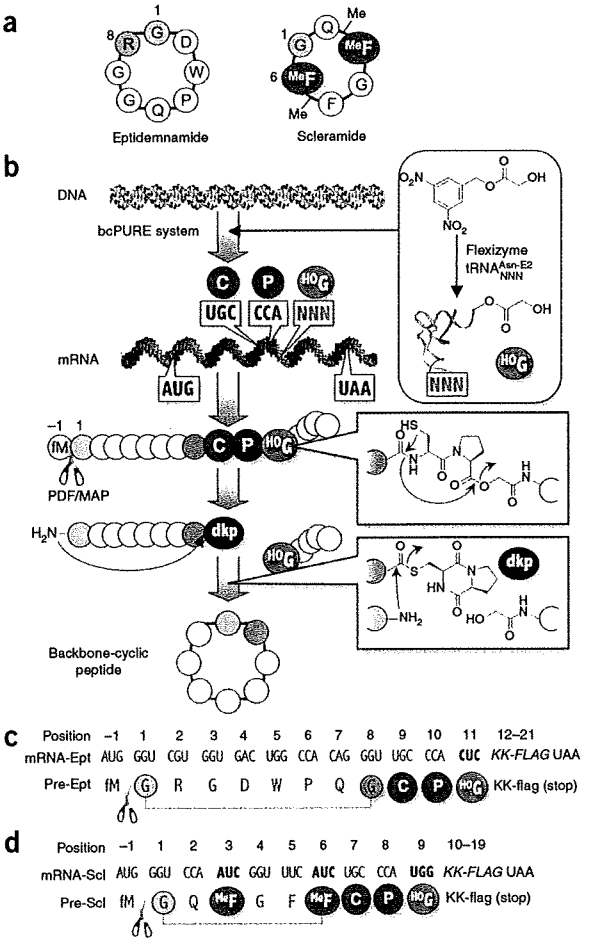

Figure 1 Ribosomal expression of backbone-cyclic peptides. (**a**) Structures of backbone-cyclic peptides expressed in this study. (**b**) mRNA-encoded expression of backbone-cyclic peptides in a withdrawn PURE system including PDF and MAP, referred to as the bcPURE system. Glycolic acid (^{HO}G) was charged onto a suppressor tRNA$^{Asn\text{-}E2}_{NNN}$ (ref. 6) using dinitro-flexizyme[8] and assigned to a vacant codon (NNN) created by withdrawing the corresponding proteinogenic amino acid. A DNA template, encoding a linear precursor peptide with a C-P-^{HO}G sequence, was transcribed and translated in the bcPURE system. This segment spontaneously rearranges to form a diketopiperadine-thioester (dkp, dark green), subsequently reacting with the N-terminal amino group at residue 1 (yellow), which is liberated by *in situ* removal of fM(−1) by PDF and MAP. These processes result in closing the backbone of residue 1 and the C-terminal residue (green). (**c**) Expression of eptidemnamide. Sequences of mRNA template (mRNA-Ept) and linear precursor peptide (pre-Ept). Number denotes the position of residue in the linear precursor peptide. ^{HO}G11 is reprogrammed to the CUC codon by the addition of ^{HO}G-tRNA$^{Asn\text{-}E2}_{GAG}$ to a leucine-withdrawn bcPURE system. KK-FLAG indicates an RNA sequence encoding the KK-flag peptide (KKDYKDDDDK). (**d**) Expression of scleramide. Sequences of the mRNA template (mRNA-Scl) and pre-scleramide (pre-Scl). ^{HO}G and *N*-methylphenylalanine (^{Me}F) are reprogrammed to the UGG and AUC codons, respectively, by the addition of ^{HO}G-tRNA$^{Asn\text{-}E2}_{CCA}$ and ^{Me}F-tRNA$^{Asn\text{-}E2}_{GAU}$ to a tryptophan/leucine-withdrawn bcPURE system.

[1]Department of Chemistry and Biotechnology and [2]Department of Advanced Interdisciplinary Studies, Graduate School of Engineering, The University of Tokyo, Tokyo, Japan. [3]Research Center for Advanced Science and Technology, The University of Tokyo, Tokyo, Japan. [4]These authors contributed equally to this work. Correspondence should be addressed to H.S. (hsuga@rcast.u-tokyo.ac.jp).

Received 15 April; accepted 11 September; published online 25 October 2009; doi:10.1038/nchembio.259

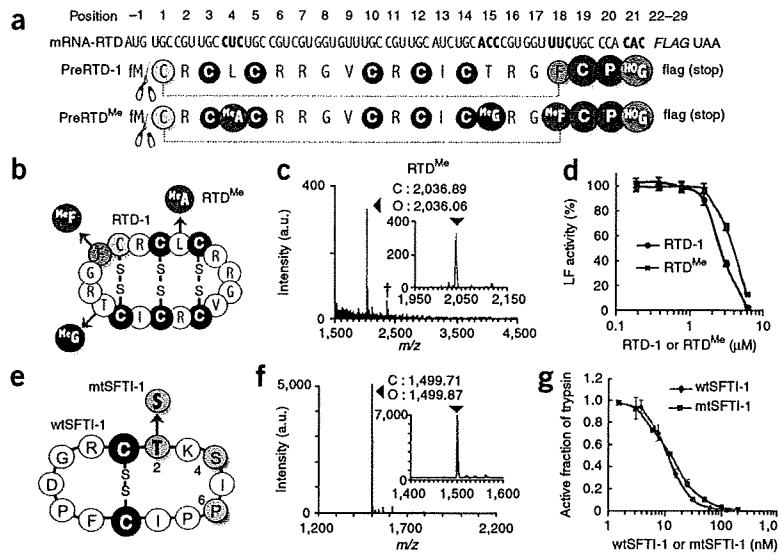

Figure 2 One-pot expression of RTD-1, its N-methylated analog RTD^{Me}, and SFTI-1. (**a**) Sequences of mRNA template (mRNA-RTD) expressing linear pre-peptides (preRTD-1 and preRTD^{Me}). For the expression of RTD-1, ^{HO}G is reprogrammed to the CAC codon by adding ^{HO}G-tRNA$^{Asn\text{-}E2}_{GUG}$ to a histidine-withdrawn bcPURE system. For RTD^{Me} expression, ^{HO}G, ^{Me}A (10), ^{Me}G (11) and ^{Me}F are reprogrammed by adding ^{HO}G-tRNA$^{Asn\text{-}E2}_{GUG}$, ^{Me}A-tRNA$^{Asn\text{-}E2}_{GAG}$, ^{Me}G-tRNA$^{Asn\text{-}E2}_{GGU}$ and ^{Me}F-tRNA$^{Asn\text{-}E2}_{GAA}$ to a bcPURE system lacking histidine, leucine, threonine and phenylalanine. RTD-1 and RTD^{Me} were expressed in one pot from the DNA templates via preRTD-1 and preRTD^{Me}, respectively (**Supplementary Fig. 4a,b**). (**b**) Structure of RTD-1 and RTD^{Me}. (**c**) MALDI-TOF spectrum of RTD^{Me}. Arrowhead indicates a peak of a singly charged species $[M+H]^{+1}$ with the observed mass (O) along with the calculated mass (C). † denotes an unknown background peak obtained in the absence of the template DNA for mRNA-RTD. (**d**) Activity of anthrax lethal toxin protease titrated as a function of the concentration of RTD-1 (blue) or RTD^{Me} (red). Error bars are s.d. based on triplicate samples. (**e**) Structure of wild-type SFTI-1 (wtSFTI-1) and mutant SFTI-1 (mtSFTI-1). Residues in positions 4 and 6 (green) were found to be wild type, whereas residue 2 (orange) contained a T→S mutation. (**f**) MALDI-TOF spectrum of the mtSFTI-1 expressed in the bcPURE system. (**g**) Activity of trypsin titrated as a function of the concentration of wtSFTI-1 (purple) or mtSFTI-1 (red). Error bars are s.d. based on triplicate samples.

cyclization. We have previously demonstrated the incorporation of ^{HO}G (1) into a peptide chain using a reprogrammed genetic code[6], creating a technical foundation for the ribosomal expression of C-P-^{HO}G segment–containing peptides. Unlike synthetic peptides, ribosomally expressed peptides typically begin with a formylated methionine (fM, 2). We anticipated that recombinant peptide deformylase (PDF) could remove the N-terminal formyl group and methionine aminopeptidase (MAP) could cleave the resultant methionine residue to generate a free N terminus of any desired amino acid. Our combined translation system is referred to as the bcPURE (backbone-cyclic peptide synthesis using recombinant elements) system, where certain proteinogenic amino acids are withdrawn from the ordinary PURE system[7] to make vacant codons, while PDF and MAP facilitate *in situ* generation of N-terminal amino-peptides and thus cyclization (**Fig. 1b**). The system makes use of flexizymes—highly flexible tRNA acylation ribozymes—to charge ^{HO}G and nonproteinogenic amino acids onto any desired tRNAs[8,9] and assign these residues to vacant codons. The integration of the bcPURE system and flexizymes provides a general platform for the production of cyclized, highly diverse peptides.

To build the foundation of this methodology, we first investigated whether dkp-thioester formation and PDF/MAP could function in the bcPURE system (**Supplementary Results** and **Supplementary Methods**). Initial studies using model peptides established several aspects of the method: (i) expression of a Cys-Pro-^{HO}G segment successfully resulted in a non-enzymatic self-arrangement to the corresponding dkp-thioester (**Supplementary Fig. 1**), (ii) the combination of PDF and MAP served to remove the N-terminal fM residue from peptides containing 7 different amino acids in the neighboring site (position 1) (**Supplementary Fig. 2a,b**) and (iii) initiation codon reprogramming[10] in combination with PDF allowed the use of 7 additional residues as initiating amino acids, yielding further diversity at position 1 and bypassing the requirement for methionine (**Supplementary Fig. 2c,d**). These aspects, which can all be achieved *in situ* with the bcPURE system, will enable the design of any desired peptide by varying the connection site to assign the first residue as one of the 14 validated options (**Fig. 1b**).

To verify whether our methodology works as planned, two monocyclic backbone-cyclic peptides, eptidemnamide (3)[11] and scleramide (4)[12] (**Fig. 1a**), were chosen as the first set of synthetic targets. Eptidemnamide was retro-connected at the site between two glycine residues (G1 and G8; the number denotes the residue position), and the corresponding mRNA was designed to express the hexameric peptide followed by the C9-P10-^{HO}G11-KK-flag segment, where ^{HO}G11 was assigned by the CUC leucine codon (**Fig. 1c**, mRNA-Ept). This mRNA was then translated using the bcPURE system in the presence of 2,2-dithiodiethanol (DTDE) to trap the pre-cyclized intermediate as a 2-mercaptoethanol adduct (see **Supplementary Fig. 1** for more information). The resulting product was subsequently treated with DTT during the flag purification to remove the 2-mercaptoethanol group. MALDI-TOF analysis of the isolated product gave a single major peak consistent with the expected molecular mass of the linear pre-peptide (**Supplementary Fig. 3a,c**, pre-Ept). The pre-Ept was then incubated in a pH 8.0 buffer with thiophenol. A MALDI-TOF analysis of the resulting product showed a single major peak with a mass that agreed with the mass value of eptidemnamide (**Supplementary Fig. 3b,d**).

Unlike eptidemnamide, which consists of only proteinogenic amino acids, scleramide contains two *N*-methylphenylalanine (^{Me}F, 5) residues. To incorporate the ^{Me}F residues into the specific positions[13], the AUC isoleucine codon was reprogrammed to ^{Me}F and the UGG tryptophan codon was reprogrammed to ^{HO}G to express the C-P-^{HO}G segment. Accordingly, we prepared the corresponding mRNA (**Fig. 1d**, mRNA-Scl) where the G1 and ^{Me}F6 sites were retro-connected, and performed ribosomal expression of the linear peptide (**Fig. 1d**, pre-Scl) in a bcPURE system containing ^{Me}F-tRNA$^{Asn\text{-}E2}_{GAU}$ and ^{HO}G-tRNA$^{Asn\text{-}E2}_{CCA}$. Following the same procedure as in the eptidemnamide synthesis, MALDI-TOF analysis of the intermediate and cyclic peptides confirmed the peaks for pre-Scl and scleramide (**Supplementary Fig. 3e–h**). These two demonstrations show the applicability of the bcPURE system integrated with flexizymes to the ribosomal expression of distinct backbone-cyclic peptides.

Rhesus-θ defensin-1 (RTD-1, 6), which belongs to a family of tetracyclic θ-defensins[14], consists of three internal dithio bridges on

the ring structure (**Fig. 2a,b**). We envisioned that we could further promote cyclization by placing a cysteine residue at the N terminus, allowing an exchange from the dkp-thioester to the C1-thioester, and leading to spontaneous rearrangement from the C1-thioester to the free amine to create the cyclic backbone[15] (**Supplementary Fig. 4a**). We therefore planned the ribosomal synthesis of RTD-1 via the backbone ligation between C1 and F18 (**Fig. 2b** and **Supplementary Fig. 4a**); at the C terminus, the segment of C19-P20-^{HO}G21-flag peptide was expressed, where ^{HO}G21 was assigned to the CAC histidine codon (**Fig. 2a**, mRNA-RTD and pre-RTD-1). In addition to wild-type RTD-1, we designed an RTD-1 analog containing three *N*-methyl amino acids, ^{Me}A4, ^{Me}G15 and ^{Me}F18, which were reassigned to the CUC leucine, ACC threonine and UUC phenylalanine codons[13], respectively (**Fig. 2a,b** and **Supplementary Fig. 4b**, RTD^{Me}, 7). Expression of these peptides was executed in the one-pot bcPURE system with DTT instead of DTDE to avoid disulfide trapping, and the MALDI-TOF analysis of the respective peptides revealed the expected molecular mass with the reduced form (**Supplementary Fig. 4c**). The *in situ* formation of disulfide bridges was achieved by prolonging the translation reaction time via air oxidation, confirmed by a loss of 6 mass units from the reduced form of RTD-1 (**Supplementary Fig. 4d** and **Fig. 2c** for RTD-1 and RTD^{Me}, respectively) and no change in their mass after treatment of the product with 2-iodoacetoamide (data not shown). We also verified the inhibitory activity of RTD-1 and RTD^{Me} against anthrax lethal toxin protease (LF) using a fluorogenic substrate (**Supplementary Fig. 4e**)[16]. Their apparent half-maximal inhibitory concentration (IC_{50}) values were determined to be approximately 2.7 and 4.0 μM, respectively (**Fig. 2d**), which were nearly identical to the previously reported value, 2.4 μM, determined for authentic RTD-1 (ref. 16). These results suggest that the correct disulfide bridges in RTD-1 and RTD^{Me} are very likely formed. Importantly, the *N*-methyl backbone modification in RTD^{Me} did not perturb the intrinsic inhibitory activity of RTD-1. This demonstrates the usefulness of our methodology for rapid explorations of backbone and side chain modifications of natural peptides in order to alter or improve their properties.

Sunflower trypsin inhibitor-1 (SFTI-1, 8) is a serine protease inhibitor consisting of a 14-mer backbone-cyclic peptide with a single disulfide bridge (**Fig. 2e**)[17]. We chose this bicyclic peptide scaffold to build the technical foundation for the library synthesis and rapid screening of bioactive sequences integrated with limiting-dilution PCR deconvolution[18,19]. First, the wild-type SFTI-1 (wtSFTI-1) was expressed in the bcPURE system under the assignment of the CUC leucine codon to ^{HO}G (**Supplementary Fig. 5a–c**), and its trypsin inhibitory activity was confirmed using a fluorogenic substrate (**Supplementary Fig. 5d**, and also see below). We then constructed a DNA library encoding SFTI-1 mutants in which three amino acid residues at positions 2, 4 and 6 embedded in the trypsin-binding loop were randomized by inserting NNK triplets into the corresponding positions in the parental DNA template (N = G, A, C or T and K = T or G) (**Supplementary Figs. 6a** and **7a**). Based on the verified protocol (**Supplementary Fig. 6b–f**), we performed a 96-well parallel one-pot expression from PCR-amplified DNA libraries originating from approximately 60 unique sequences, and directly transferred the translation mixture in each well to the trypsin inhibition assay (**Supplementary Fig. 7b**). We performed a total of three rounds of screening and deconvolution of active sequences (**Supplementary Fig. 7c,d**; see details in **Supplementary Results**), identifying one mutant SFTI-1, referred to as mtSFTI-1 (9), with a T2S mutation (**Fig. 2e,f**). A titration of the activity as a function of mtSFTI-1 concentration resulted in an IC_{50} value of 13.4 ± 0.7 nM (K_i = 13 ± 1 nM, determined by fitting to the Morrison's slow-tight binding equation; **Fig. 2g**), which was comparable to that of wtSFTI-1 (IC_{50} = 12.1 ± 0.3 nM and K_i = 8 ± 1 nM)[17]. Thus, integration of the ribosomal expression of a library SFTI-1 with activity screening and limiting-dilution PCR deconvolution enables rapid determination of active sequences.

Our proof-of-concept studies reported here have established a unique enabling methodology for the synthesis and discovery of backbone-cyclic peptides for potential therapeutic uses. Importantly, all processes—including transcription of the DNA template, translation of the peptide, generation of the N-terminal amino group, formation of the dkp-thioester and N-C termini cyclization—take place in one pot using the bcPURE system. This feature has enabled us to readily prepare and analyze a library of backbone-cyclic peptides based on a bicyclic scaffold. Although the screening/deconvolution methodology reported here is limited in that it can only be applied to rather small libraries ($<10^5$ molecules)[18,19], it is inexpensive, easy and widely applicable to various *in vitro* assay methods. We envision that the combination of an *in vitro* display[20,21] with the screening/deconvolution methodology will offer a rapid and reliable means for identification of functional peptides. Another important feature of our method is the ability to incorporate nonproteinogenic amino acids into peptide chains at multiple sites[6,8,13,22–24]. This is in sharp contrast to other mRNA-directed backbone-cyclic peptide expression methods, such as those using inteins[15,25], and as such should accelerate the discovery of new classes of peptides.

Note: Supplementary information and chemical compound information is available on the Nature Chemical Biology website.

ACKNOWLEDGMENTS

This work was supported by grants from the Japan Society for the Promotion of Science (JSPS) Grants-in-Aid for Scientific Research (16101007) and a research and development project of the Japanese Industrial Science and Technology Program in the New Energy and Industrial Technology Development Organization (NEDO) to H.S. T.K. and A.O. are supported by JSPS Research Fellowships for young scientists (20-664 and 19-1722, respectively).

AUTHOR CONTRIBUTIONS

T.K., A.O. and H.S. designed the project. T.K., A.O., M.O., H.A. and H.M. performed experiments. The manuscript was written by T.K., A.O. and H.S.

Published online at http://www.nature.com/naturechemicalbiology/.
Reprints and permissions information is available online at http://npg.nature.com/reprintsandpermissions/.

1. Trabi, M. & Craik, D.J. *Trends Biochem. Sci.* **27**, 132–138 (2002).
2. Kohli, R.M. & Walsh, C.T. *Chem. Commun. (Camb.)* 297–307 (2003).
3. Tang, Y.Q. *et al. Science* **286**, 498–502 (1999).
4. Ladner, R.C. *Trends Biotechnol.* **13**, 426–430 (1995).
5. Kawakami, T. & Aimoto, S. *Chem. Lett.* **36**, 76–77 (2007).
6. Ohta, A., Murakami, H., Higashimura, E. & Suga, H. *Chem. Biol.* **14**, 1315–1322 (2007).
7. Shimizu, Y. *et al. Nat. Biotechnol.* **19**, 751–755 (2001).
8. Murakami, H., Ohta, A., Ashigai, H. & Suga, H. *Nat. Methods* **3**, 357–359 (2006).
9. Ohuchi, M., Murakami, H. & Suga, H. *Curr. Opin. Chem. Biol.* **11**, 537–542 (2007).
10. Goto, Y. *et al. ACS Chem. Biol.* **3**, 120–129 (2008).
11. Donia, M.S. *et al. Nat. Chem. Biol.* **2**, 729–735 (2006).
12. Whyte, A.C., Joshi, B.K., Gloer, J.B., Wicklow, D.T. & Dowd, P.F. *J. Nat. Prod.* **63**, 1006–1009 (2000).
13. Kawakami, T., Murakami, H. & Suga, H. *Chem. Biol.* **15**, 32–42 (2008).
14. Selsted, M.E. *Curr. Protein Pept. Sci.* **5**, 365–371 (2004).
15. Kimura, R.H., Tran, A.T. & Camarero, J.A. *Angew. Chem. Int. Edn Engl.* **45**, 973–976 (2006).
16. Wang, W. *et al. J. Biol. Chem.* **281**, 32755–32764 (2006).
17. Korsinczky, M.L., Schirra, H.J. & Craik, D.J. *Curr. Protein Pept. Sci.* **5**, 351–364 (2004).
18. King, R.W., Lustig, K.D., Stukenberg, P.T., McGarry, T.J. & Kirschner, M.W. *Science* **277**, 973–974 (1997).
19. Rungpragayphan, S., Nakano, H. & Yamane, T. *FEBS Lett.* **540**, 147–150 (2003).
20. Roberts, R.W. & Szostak, J.W. *Proc. Natl. Acad. Sci. USA* **94**, 12297–12302 (1997).
21. Ueno, S., Arai, H., Suzuki, M. & Husimi, Y. *Int. J. Biol. Sci.* **3**, 365–374 (2007).
22. Forster, A.C. *et al. Proc. Natl. Acad. Sci. USA* **100**, 6353–6357 (2003).
23. Kawakami, T., Murakami, H. & Suga, H. *J. Am. Chem. Soc.* **130**, 16861–16863 (2008).
24. Ohta, A., Yamagishi, Y. & Suga, H. *Curr. Opin. Chem. Biol.* **12**, 159–167 (2008).
25. Scott, C.P., Abel-Santos, E., Wall, M., Wahnon, D.C. & Benkovic, S.J. *Proc. Natl. Acad. Sci. USA* **96**, 13638–13643 (1999).

Bioorganic & Medicinal Chemistry Letters 19 (2009) 3892–3894

Contents lists available at ScienceDirect

Bioorganic & Medicinal Chemistry Letters

journal homepage: www.elsevier.com/locate/bmcl

A flexizyme that selectively charges amino acids activated by a water-friendly leaving group

Nobuyoshi Niwa [a,†], Yusuke Yamagishi [a,†], Hiroshi Murakami [b], Hiroaki Suga [a,b,*]

[a] Department of Chemistry and Biotechnology, Graduate School of Engineering, The University of Tokyo, Tokyo 113-8656, Japan
[b] Research Center for Advanced Science and Technology, The University of Tokyo, Tokyo 153-0894, Japan

ARTICLE INFO

Article history:
Received 11 February 2009
Revised 20 March 2009
Accepted 25 March 2009
Available online 28 March 2009

Keywords:
Ribozyme
In vitro selection
Non-proteinogenic amino acid
Aminoacylation

ABSTRACT

We have developed a new flexizyme (a flexible de novo tRNA acylation ribozyme) system, a pair of amino-derivatized benzyl thioester (ABT) and amino flexizyme (aFx). ABT bearing the ammonium ion was designed to render the acyl-donor substrates better water solubility. Although the previously reported flexizymes (eFx and dFx) did not show acylation activity for the ABT derivatives, a new flexizyme variant aFx, generated by in vitro selection against an amino acid activated ABT, exhibits high selectivity toward those activated ABT. The flexizymes system including aFx, eFx, and dFx enables us to prepare a wide variety of acyl-tRNAs charged with non-proteinogenic amino acids.

Engineering of the universal genetic code has given us a new opportunity to express peptides or proteins bearing non-proteinogenic amino acids.[1–4] Recent developments in methodologies of the genetic code reprogramming have enabled us to reassign multiple codons to non-proteinogenic amino acids.[5–21] By means of such methodologies, libraries of non-standard peptides can be prepared in the mRNA-encoding manner.[14] We have engaged the development of such a methodology integrated with flexizymes.[10,22–24] Flexizymes are flexible tRNA acylation ribozymes and facilitate the preparation of various non-proteinogenic aminoacyl-tRNAs, which are otherwise complex and technically difficult processes. Two flexizymes, referred to as eFx and dFx, have been devised (Fig. 1); the eFx acylates tRNA with amino or hydroxy acids upon activation with cyanomethyl ester (CME) group or *p*-chlorobenzyl thioester (CBT), where its activity relies on the recognition of aromatic sidechain or the CBT group in the substrate; on the other hand, dFx acylates tRNA with those activated with 3,5-dinitrobenzyl ester (DBE) group, where its activity fully relied on the recognition of the DBE group. Since both flexizymes bind the 3′-end sequence of tRNA via the 3-base pairing interaction (RCCA-3′, R = G, A and U are the preferable discriminator base at position 73, but even C is acceptable under prolonged incubation), any tRNAs can be the acyl-acceptor for the flexizymes. Thus, by the combination of these two flexizymes, virtually any desired acyl-tRNAs can be readily prepared.

However, a shortcoming of the current flexizyme system is that since the CBT or DBE-derived the acyl-donor substrates make them more hydrophobic, some derivatives, particularly those with hydrophobic sidechains, are occasionally difficult to dissolve in the aqueous reaction buffer. Notably, eFx and dFx are able to retain their catalytic activity in the buffer containing up to 20% and 40% DMSO, respectively, but the addition of DMSO to the reaction buffer

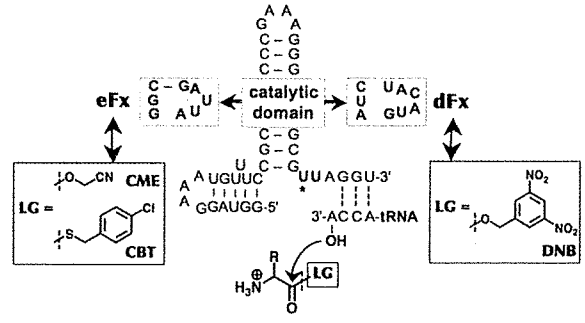

Figure 1. Flexizymes and their cognate leaving groups in substrates. Chemical structures of a benzyl ester and thioester leaving group. R represents amino acid sidechains including non-proteinogenic ones. Each flexizyme recognizes the specific leaving group and charges the acyl group onto the 3′-hydroxyl group at the tRNA 3′-end. *Abbreviations*: LG, leaving group; CME, cyanomethyl ester; CBT, *p*-chlorobenzyl thioester; eFx, enhanced flexizyme; DNB, 3,5-dinitrobenzyl ester; dFx, dinitro flexizyme. U with asterisk denotes the absolutely conserved U-turn base. Bold bases orchestrate to constitute the catalytic domain of each flexizyme.

* Corresponding author. Tel.: +81 03 5452 5495; fax: +81 3 5452 5496.
E-mail address: hsuga@rcast.u-tokyo.ac.jp (H. Suga).
† These authors contributed equally to this work.

0960-894X/$ - see front matter © 2009 Elsevier Ltd. All rights reserved.
doi:10.1016/j.bmcl.2009.03.114